NTNU – Trondheim
Norwegian University of
Science and Technology

Modeling of Water Behavior in Hydraulically-Fractured Shale Gas Wells

Sandi Rizman Hersandi

Petroleum Engineering
Submission date: July 2013
Supervisor: Curtis Hays Whitson, IPT

Norwegian University of Science and Technology
Department of Petroleum Engineering and Applied Geophysics

Sandi Rizman Hersandi

Modeling of Water Behavior in Hydraulically-Fractured Shale Gas Wells

Thesis for the degree of Master of Science

Trondheim, July 2013

Norwegian University of Science and Technology
Faculty of Engineering Science and Technology
Department of Petroleum Engineering and Applied Geophysics

NTNU – Trondheim
Norwegian University of
Science and Technology

Abstract

This study presents the modeling of water behavior in hydraulically-fractured of shale gas wells. A five layers model represents a hydraulically-fractured shale gas well was built in Sensor reservoir simulator through Pipe-It, integrated asset management software. Stress dependent permeability multiplier is applied in the model to represent the permeability enhancement in the zone close to the fracture face during the fracturing stimulation.

An implicit black-oil logarithmic model with a total of grid number of 5,800 and thickness of 200 ft is used as the base case model. The horizontal well extends through the reservoir in x-direction. The fracture is located in the center of x-axis, while the tip of the fracture is in the middle of y-axis.

Water behavior in the fracture for this study is represented by water saturation within the fracture grids. A better understanding of water behavior in the fracture and its effects on the production profile was obtained through several sensitivity cases, which include number of layers, perforation location, matrix permeability, gas production rate, and shut-in time.

Based on the sensitivity tests, it was observed that high water saturation in the fracture is found when the perforation is located in the uppermost layer of the model. For matrix permeability sensitivity, the total *kh* for the model is maintained at a constant. Reservoir with high matrix permeability in the uppermost layer gives higher water saturation in the fracture. The varying gas production rates influence the water saturation in the fracture. Higher gas rates result in higher water saturation in the fracture. The water saturation profile analysis based on the rate sensitivity shows that a critical gas rate to feed the water from the matrix to the fracture is expected to exist. Water saturation profiles in the matrix have relatively the same profile according to shut-in sensitivity. These differing water saturation profiles on the shut-in sensitivity indicate delayed of water feed from the matrix to the fracture.

Also, different perforation locations affect the water production profile, but not on the gas production profiles. Both gas and water production profiles are not significantly affected by different matrix permeability values. Rate sensitivity shows that higher gas rate results in higher total water production. Shut-In period also affects the production profiles. Gas and water productions are observed to decrease with an increased shut-in time due to the delay of production. It is noteworthy that the differences in total water productions are substantial. This is due to shut-in period after water injection reduces water recovery, as compared to immediate production after water injection.

From the sensitivities applied to the model, water saturation in the fracture is generally affected by all sensitivity parameters, thus also affects production profiles. This study contributes to having a better understanding in the water behavior in the fracture and the production profiles of shale well gas.

Acknowledgements

This project is a part of the Master of Science Program at Department of Petroleum Engineering and Applied Geophysics, NTNU, Trondheim, Norway. First and foremost, I would like to thank my supervisor, Professor Curtis H. Whitson for the opportunity given to me as his student. He has given me not only guidance and support but also his valuable comments and comprehensive feedback during working with him.

I would like to thank Dr. Aleksander Juell, Postdoc Student at NTNU and engineer at PERA A/S, for helping me to understand Pipe-It Shale Well Optimizer, for his guidance and suggestions during this study.

My appreciation also goes to Wojciech Jurus, PhD Student at NTNU, who gave me suggestions for the model. I would like to acknowledge Petrostreamz A/S for the Pipe-It license and Coats Engineering, Inc. for the Sensor license.

It is a great pleasure to thank everyone who supports me during my master study: Wynda Astutik and Dr. Silvya Dewi Rahmawati who always have discussion time for me; Indonesian community in Trondheim that make me feel like home during my study in Trondheim.

Finally, I am truly indebted to my family, for their support through endless pray.

Trondheim, July 2013

Sandi Rizman Hersandi

Table of Contents

List of Tables

List of Figures

Chapter 1

Introduction

1.1 Background

Unconventional reservoir has become more interesting since the reserves are promising and it spreads in large extent. Hydrocarbon from unconventional reservoir is still hydrocarbon composed like other hydrocarbon from conventional reservoir. Unconventional sources are usually dispersed in larger area than conventional sources.

Shale gas reservoir as one of the unconventional resources has been developed and has been studied to get a better understanding the behavior. Shale gas are deposited and trapped within shale rocks. The shale rock usually not only acts as a source but also as a reservoir. Many wells are required to develop the shale gas reservoir since the large extent of the reservoir. A combination of directional drilling and hydraulic fracturing are used to make large amounts of shale gas and/or oil reservoir accessible.

Hydraulic fracturing is the process of injecting high pressure fracturing fluids into the formation to create small cracks or fractures. These fluids typically consist of water, sand/proppant, and chemical additives. The sand/proppant keeps the fractures opened. Fractures provides pathways to allow oil or/and gas to flow into the wellbore and thus increase the production.

Fracturing fluids which is injected during fracturing process will flow back to the surface. Fields results have indicated only 15-30% of the fracturing fluid is recovered. Past studies have suggested that fracturing fluid, which is water, is trapped in the matrix near the fracture face due to high capillary pressure in the matrix [1]. There is a possibility for the water to be trapped in the fracture itself. Liquid trapped in the fracture may affect productivity of the well.

1.2 Study Objective

The main objective of this study is to model water behavior in hydraulically-fractures of shale gas wells. A shale gas reservoir with hydraulically-fractures and a horizontal well model is built. Saturation water within the fracture grids is the object of the study. Sensitivity study is conducted to understand the effect of different parameters to the water behavior within the fracture and on its production. As author knowledge, there has not been any publication presenting specific study about the modeling of water behavior in the hydraulically-fracture especially for shale gas wells.

1.3 Description of Employed Software

1.3.1 Pipe-It

Pipe-It is unique IAM (Integrated Asset Management) software to integrate models and optimize petroleum assets [6]. Pipe-It has been developed by Petrostreamz A/S, a software company developed at PERA A/S. Pipe-It allows us to chain several applications in series and parallel, launch of literally any software on any operating system. Pipe-It provides a framework to pipe together the array of software, to build and to automate integrated projects, to perform optimization across disciplines, and to do compositional streams from black-oil rates [6]. Its principle is to send stream of information from a resources through a process into another resource.

A Pipe-It project consists of three basics building blocks, which are the Resources, the Process, and the Connectors. Sockets and Composite are other Pipe-It features.

MapLinkz and Linkz, is features in Pipe-It, has a function to connect the same data in different resources. It will give better working efficiency because we only have to change the parameter in one file and the same parameter in other files will be automatically updated. It is used to avoid lots of manual copy and paste work which time consuming.

Pipe-It has many functional features to work series or parallels using different kind of software. Conversion from one software output file to a file which is suitable for other software is easy to be done. For example, output from different reservoir simulators can be combined to be one file easily.

Other important feature in Pipe-It is Optimizer. An entire Pipe-It Project can be run time-and-again with changes to any input data using the Optimizer.

In this study, Pipe-It was used for running the chronology of the defined process. Pipe-It made the work easier since all the program is run at the same windows and automatically follows the chronology that has been made. Pipe-It was used to simplify the Sensor run and to connect different kind of input/include files, for example; it was used to link Excel file and Sensor include files.

1.3.2 Sensor

Sensor, which stands for System for Efficient Numerical Simulation of Oil Recovery, is compositional and black oil reservoir simulation software developed by Coats Engineering, Inc. *This software is a generalized 3D numerical model used by engineers to optimize oil and gas recovery processes through simulation of compositional and black oil fluid flow in single porosity, dual porosity, and dual permeability petroleum reservoirs* [3]

Impes and Implicit formulations are included in Sensor. There are three linear solvers available; reduced bandwidth direct (D4), Orthomin preconditioned by Nested Factorization, and Orthomin preconditioned by ILU (red black and residual constraint options). The gridding in Sensor is flexible as it can handle any grid type or combination of grid types. For the compositional simulation in Sensor, Equations of State (EOS) of the Peng-Robinson (PR) and Soave-Redlich-Kwong (SRK) are used, included the optional shift factors and any number components.

Sensor6k is a restricted version of Sensor. Problems containing less than 6000 active grid blocks can be simulated by Sensor6k. This version is proposed to students and to non-profit organizations. Sensor can be launched either from a command prompt or by other applications. In this study, not only Sensor6k was utilized but also Full version of Sensor was used to run the model with grid more than 6000.

By all these functionalities, in this study Sensor was used to make a layered shale gas reservoir model with a hydraulically-fracture and a horizontal well. Sensor is also used to run the model. Water saturation and production data from Sensor simulation were extracted to understand the water behavior and its effect on production.

1.3.3 Tecplot RS

Tecplot RS is software from Tecplot, Inc. The software can visualize the reservoir simulation results. Tecplot RS has ability to visualize Sensor output file, both the plot and the grid. In this

study, the software was used to compare different result of different cases. Fluid movement in the model was also observed using 3D grid option in Tecplot RS. It helps to get a better understanding on water behavior in the fracture from different cases using the model visualization. Tecplot RS 2012 version is used throughout the study.

Chapter 2

Model Initialization

2.1 Model Preparation

The objective of this study is to model the water behavior in a hydraulically-fracture of shale gas well. Water saturation in the fracture and its production profile were analyzed. Thus, a base case model was generated to represent a shale gas well.

A model represents shale gas reservoir with fractures and a horizontal well was built using Sensor through Pipe-It. A Pipe-It project called Pipe-It Shale Well Optimizer was used in this study. Pipe-It Shale Well Optimizer will be explained further in the next sub-chapter. The reservoir has 5,000 ft in horizontal length well section, 200 ft in thickness, 160 acre in well spacing, and 10 fractures along the horizontal section. The model is a fully implicit model. Logarithmic gridding from the default fracture tip to the wellbore and from the fracture tip to the y-direction of the model were used for the grid type. The grid was also refined at the fracture tip and coarsens away from the tip. In this study, the model is called as the base case model.

Only a half fracture zone was modeled in this study due to symmetrical model. Each fracture behaves independently, so that only one side of the fracture needs to be modeled. The model uses total number of grid of 5,800 (N_x=29, N_y=40, N_z=5). The horizontal well extends through the reservoir in x-direction. **Figure 2.1** shows the model has been built using Sensor through Pipe-It Shale Well Optimizer. The fracture is located in the center of x-axis (I=15). The tip of the fracture is in the middle of the y-axis (J=20).

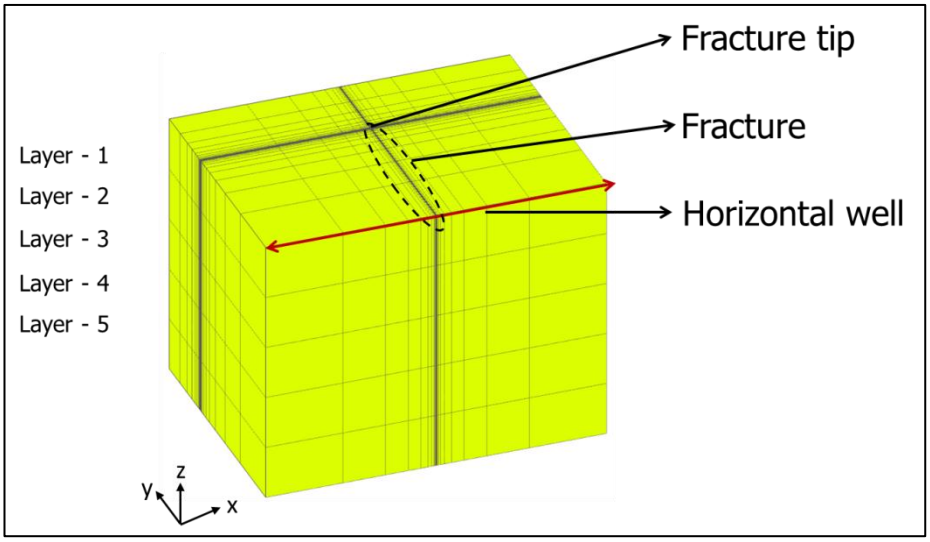

Figure 2. 1 – Reservoir Model

2.2 Pipe-It Shale Well Optimizer

A Pipe-It project called Pipe-It Shale Well Optimizer was used in this study. It is developed by Dr. Aleksander Juell, Postdoc Student at NTNU and engineer at PERA A/S. Pipe-It Shale Well Optimizer provides modeling capabilities in shale and ultra-tight gas well.

In Pipe-It Shale Well Optimizer, there are three modules:

1. Well model, including liquids-rich pressure/volume, and PVT phase behavior fluid description),
2. Production history matching,
3. Well design optimization, including economics model optimization.

Pipe-It Shale Well Optimizer was modified in intention to have reservoir model which suit with the study. Layering Option for the model has been added to Grid Definition section in Pipe-It Shale Well Optimizer. As shown in **Figure 2.2**, three parameters, which include thickness, permeability, and porosity, has been added in Layering Option. This additional feature has been added to see the effect of layering model and to accommodate the study on heterogeneity of the reservoir. Five layers of the reservoir have been applied as the base case model. In the base case model, each layer has the same properties in thickness, permeability and porosity.

```
! ----------------- Layers ----------------------
! If you need a 3D model with layering in the
! z-direction, this section must be present.
! Each layer is added as a new line between the
! LAYERS and END LAYERS keywords.
! Each layer must have the following data entries:
! thickness, permeability, porosity.
! Values entered with the THICKNESS, POROSITY,
! and PERMEABILITY keywords are ignored.
! -----------------------------------------------
LAYERS
! h (ft)   k (md)  phi
40      0.0002  0.1
40      0.0002  0.1
40      0.0002  0.1
40      0.0002  0.1
40      0.0002  0.1
END LAYERS
```

Figure 2. 2 – Layering Option in Grid Definition (e.g. The Base Case Model)

The stress dependent permeability also has been added to the Pipe-It Shale Well Optimizer. The stress dependent permeability modifiers (tables) are used in most of the reservoir simulators. It has been used in the reservoir simulators to model the permeability reduction during production period.

In this study, it was added to represent the permeability enhancement around the fractured zone during fracturing stimulation. It shows the relation between stress and permeability during fracture stimulation treatment.

The stress dependent permeability multiplier, k/k_o , is calculated from **Equation (2.1)** [5]. Exponent *m*, permeability enhancement factor, depends on matrix porosity, fracture conductivity, maximum injection bottomhole pressure, and fracture half length (Jurus, 2013). The net pressure, p_{net}, is the difference between current cell pressure and initial cell pressure.

$$\frac{k}{k_o} = 10^{mp_{net}} \qquad (2.1)$$

The model does not describe the real physics of the changes that take place in the zone close to the fracture face. However, it allows describing the overall effect of the permeability increase with permeability enhancement factor (exponent *m*). In this study, water injection process represents the fracturing stimulation in the reservoir simulator. The injectivity of the well is controlled by the parameter *m*. *With appropriate magnitude of m the real injection rates and volumes can be honored in the reservoir simulator model* [5]

The stress dependent permeability modifiers are only applied when the pressure is higher than the original reservoir pressure (water injection treatment). The permeability equals the

given original value and is assumed constant for pressure below the original reservoir pressure, for e.g. during production. *The maximum allowed value of the multiplier for permeability increase is 10^6, and model calculated values exceeding this threshold are set to the value of 10^6* [5].

In the model, the stress dependent permeability changes were applied for both fracture and matrix. The same permeability enhancement factor was used for matrix cells in x, y and z-direction and for fracture cells in x-direction (across fracture face). The permeability of the fracture in y and z-direction increased according to a model with different permeability enhancement factor.

In the Pipe-It Shale Well Optimizer, the stress dependent permeability multiplier is linked with well.inc. The file well.inc is a file contains of the Bottomhole Pressure (BHP) constraint, both production and injection. The value of BHP injection is linked with the excel file to generate the include file (stress.inc) contains the stress and permeability multiplier.

Chapter 3

Modeling of Water Behavior in the Fracture

3.1 The Base Case Model Description

The model, which built using Sensor via Pipe-It Shale Well Optimizer, was used as the base case model. Dry gas with specific gravity of 0.7 was used in this study. The compositions of the gas can be seen at **Table 3.1**. A conversion from compositional to black oil was done for this study. The z-factor was calculated using Hall-Yarborough equation. It used to calculate gas formation volume factor. Lee-Gonzales equation was used to calculate gas viscosity. **Figure 3.1** shows its values varying with pressure.

Table 3.2 provides reservoir data which was used in the base case model. Reservoir model has 200 ft total thickness and it is divided into 5 layer with each layer has the same thickness, which is 40 ft. The matrix permeability is 0.0002 md. At the base case model, only the uppermost layer was perforated. A horizontal well section was completed along the x-direction.

As mentioned before, only a half fracture zone was modeled in this study because of symmetry and each fracture behaves independently. The well rate equals twice the half-model rate time the total number of fractures [9].

Fracture conductivity is 1,000 md-ft in this study. The fracture permeability was calculated based on fracture conductivity. The fracture pore volume in this model is based on 0.25 porosity and a fracture width 0.01 ft. *The numerical fracture width may be 0.1 or even 1 ft*

without having any real impact on results, as long as actual fracture conductivity and volume are honored [9].

Table 3. 1 – Gas Compositions

Component	Composition (mole percent)
N_2	0.01
CO_2	0.03
C_1	86
C_2	5.16
C_3	4.25
iC_4	1.1
nC_4	1.4
iC_5	0.8
nC_5	0.6
C_6	0.55
C_{7+}	0.1
M C_{7+}	113
SG Gas	0.7

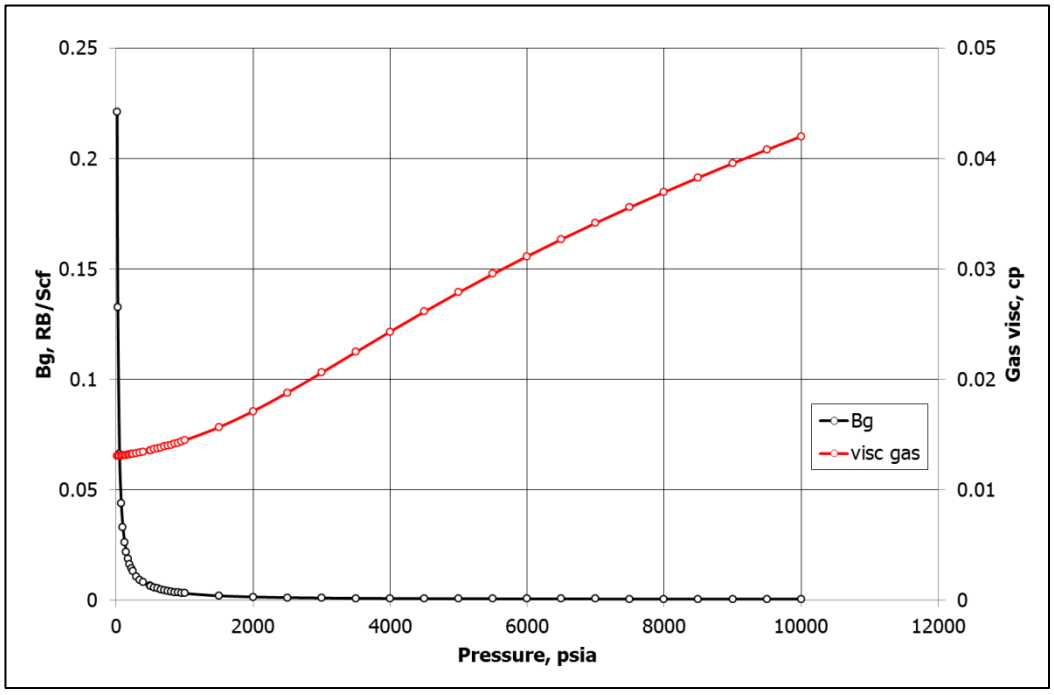

Figure 3. 1 – Gas Formation Volume Factor and Gas Viscosity

Fracture porosity, was calculated using **Equation (3.1)**. By using fracture width model 0.083 ft, the fracture porosity is 0.03. Followed **Equation (3.2)**, fracture permeability model is ~12,000 md.

$$frac.porosity\ model = \frac{frac.porosity\ physical \times frac.width\ physical}{frac.width\ model} \quad (3.1)$$

$$frac.permeability\ model = \frac{frac.conductivity\ physical}{frac.width\ model} \quad (3.2)$$

Table 3. 2 – Base Case Model Descriptions

RESERVOIR AND WELL GEOMETRY	Value	Unit
Number of grids in x-direction, N_x	29	
Number of grids in y-direction, N_y	40	
Number of grids in z-direction, N_z	5	
Initial Reservoir Pressure, P_R	5,000	psia
Depth to the top reservoir	10,000	ft
Well spacing, A	160	acre
Reservoir thickness, h	200	ft
Horizontal well length, L_h	5,000	ft
Number of fracture, N_f	10	
Reservoir temperature	200	^oF
Wellbore diameter - vertical section, r_{wv}	4.67	inch
Wellbore diameter - horizontal section, r_{wh}	4.67	inch
MATRIX PROPERTIES	Value	Unit
Matrix permeability, k_m	0.0002	md
Matrix porosity, φ_m	0.1	
Permeability enhancement factor, m	0.00115	psi^{-1}
FRACTURE PROPERTIES	Value	Unit
Fracture width	0.083	ft
Fracture conductivity	1,000	md-ft
Fracture porosity, φ_f	0.03	
Fracture half length, x_f	300	ft
Permeability enhancement factor, m	0.00065	psi^{-1}

Figure 3.2 shows relative permeability curves for matrix and fracture used in the model. Traditional rock relative permeability is assumed applicable to shale. Saturation exponent of 2.5 was used for the matrix, while the fracture used linear relationship.

Table 3. 3 – Relative Permeability and Capillary Pressure Analytical Data

Parameter	Matrix	Fracture
Connate water saturation, S_{wc}	0.2	0
Critical gas saturation, S_{gc}	0.2	0
Rel. perm. of water, $k_{rw}(1-S_{gc})$	1	1
Rel. perm. of gas, $k_{rg}(S_{wc})$	1	1
Rel. perm exponents, $n_w = n_g$	2.5	1
a_1; a_2; a_3	0 ; 3,480 ; 5	-
b_1; b_2; b_3; b_4; b_5	0 ; 3,480 ; 5 ; 0 ; 0	-

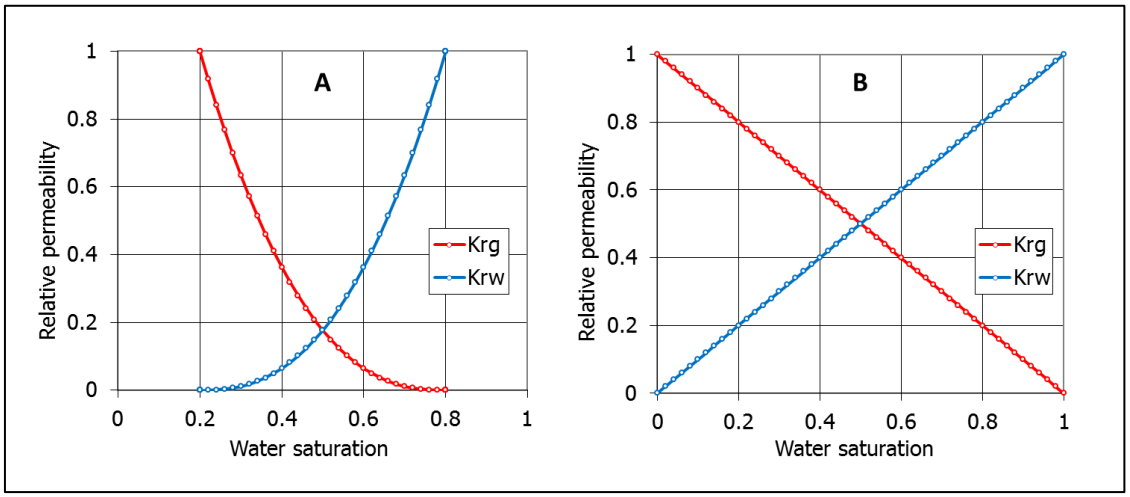

Figure 3. 2 – Relative Permeability Curves for Matrix (A) and Fracture (B)

For capillary pressure, correlation parameter values used for the model are found in **Table 3.3**. With gas-water interfacial tension of 60 mN/m and 5 nm pore radius at S_{wc}, it gives maximum capillary pressure of 3,480 psi. It is only applied for the matrix. No capillary pressure is applied to the fracture. Drainage and imbibition capillary pressure, P_{cgwD} and P_{cgwI}, are calculated using the default from Sensor reservoir simulator used in this study. According to **Equation (3.3)** and **Equation (3.4)**, is defined as functions of normalized water saturation (S_{wn}).

$$P_{cgwD} = a_1 + a_2 * (1 - S_{wn})^{a_3} \quad (3.3)$$

$$P_{cgwI} = b_1 + b_2 * (1 - S_{wn})^{b_3} - b_4 * S_{wn}{}^{b_5} \quad (3.4)$$

$$S_{wn} = (S_w - S_{wc})/(1 - S_{wc}) \quad (3.5)$$

A macro excel file for generating the stress dependent permeability multiplier is connected to an include file which contains a value of initial reservoir pressure and maximum injection bottomhole pressure. The output file contains stress dependent permeability multiplier used in this study. The stress dependent permeability multiplier is only applied when the water

injection is performed. **Figure 3.3** shows the permeability multipliers for this matrix with an initial pressure 5,000 psia, using a slope m = 0.00115.

The permeability for the matrix in x-, y-, and z-direction are modified during water injection. The modification in the fracture is only applied in y-, and z-direction. While in x-direction it follows modification for the matrix in x-direction as seen in **Figure 3.4**. For the fracture, a slope m = 0.00065 is used.

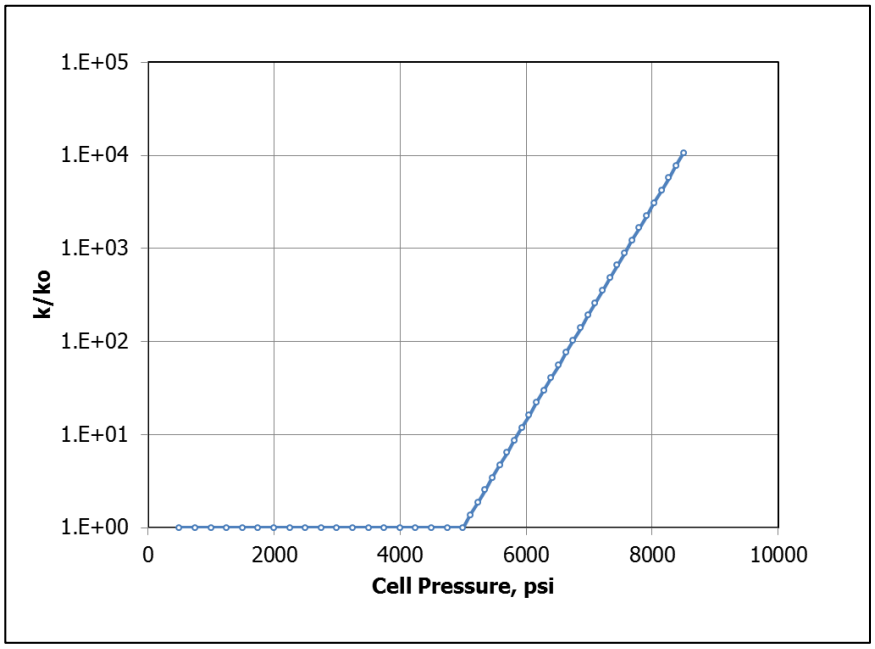

Figure 3. 3 – Stress Dependent Permeability Model for Matrix

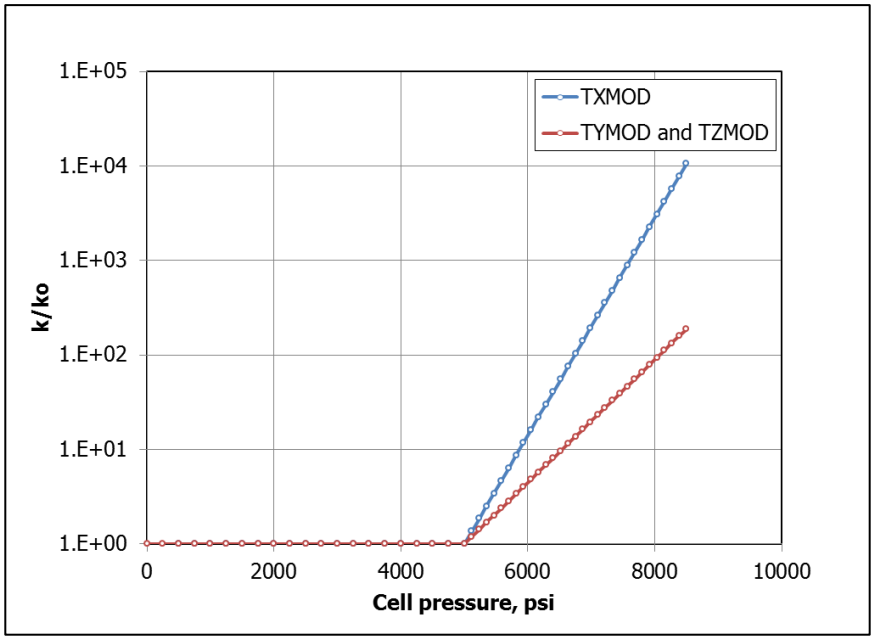

Figure 3. 4 – Stress Dependent Permeability Model for Fracture

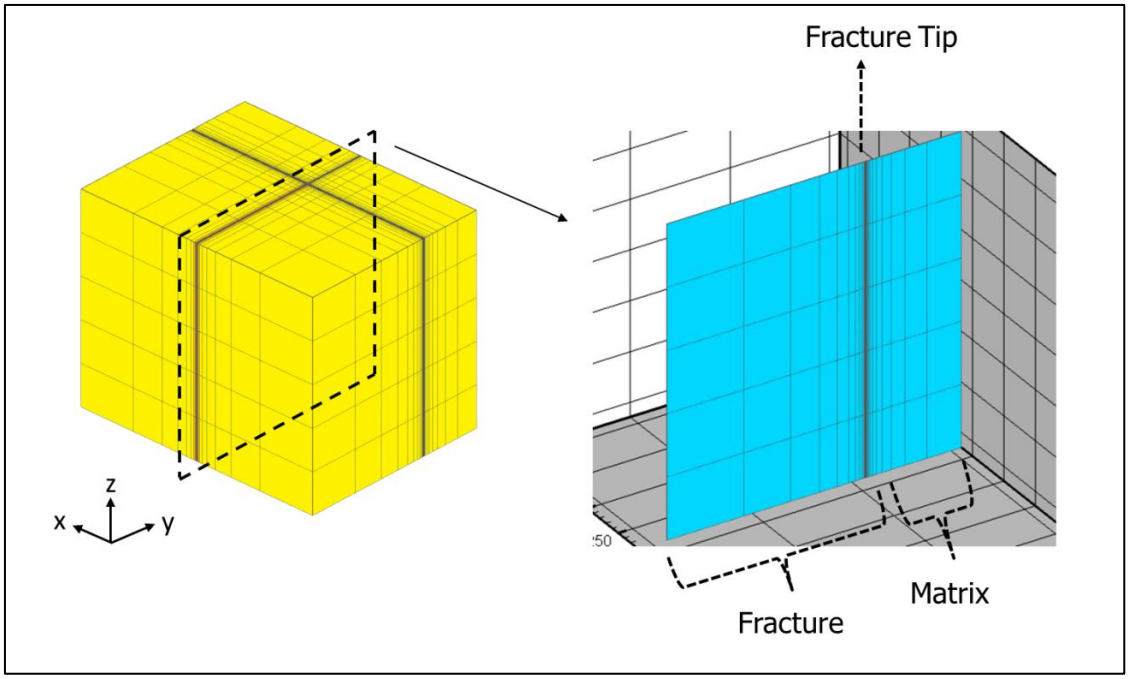

Figure 3. 5 – Slice of Grid for Water Saturation Analysis in the Fracture

The model was simulated for 200 days. Initial water saturation in the matrix is 0.2. To simulate fracturing stimulation, water injection was performed. Amount of 320,000 bbl/d water was injected to the reservoir for 3 hours. It means 2,000 bbl water was injected to a model (half-fracture model). The maximum injection bottomhole pressure is 8,000 psi.

Water saturation was only analyzed for the fracture. A slice of fracture grid in the model is the object of the study. It can be seen in **Figure 3.5**. The fracture is located in the middle of the model, which is I=15. **Figure 3.6** shows water saturation snapshot in JK-cross section at I=15 for the base case model at time 0.125 days (A), 50 days (B), 100 days (C), and 200 days (D). We can see how water behaves with time in the fracture.

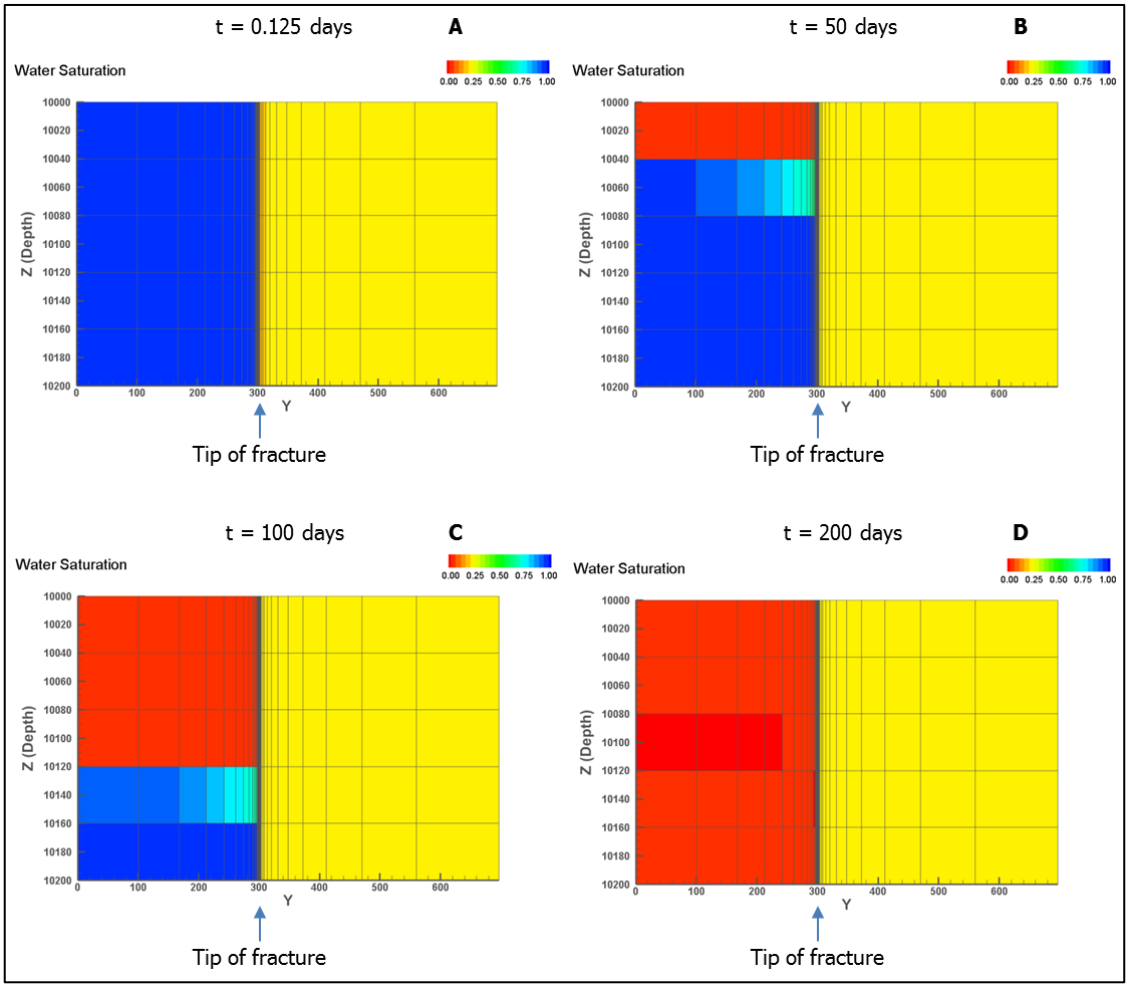

Figure 3. 6 – Base Case: Water Saturation Snapshot (JK-cross section, I=15)

3.1.1 Water Saturation within the Fracture

Figure 3.7 until **Figure 3.11** show water saturation value at the same position as the snapshot. In this plot, water saturation profile is observed to the y-direction. The water saturation at the end of water injection, which is at t=0.125 days, is very high in the fracture. Fracture is filled with the water. Water segregation due to gravity force is observed during water injection, so that water fills the bottom layer first although water is injected through the uppermost layer. Water also imbibes into the formation. It can be seen water saturation in grid J>20, which the matrix grid, increase (S_w>0.2). Water saturation in the fracture decreases with production. From **Figure 3.7**, the uppermost layer of the fracture which is layer-1 has no water after 50 days of production until the end of simulation.

Along with production, water saturation in layer-2 and layer-3 of the fracture decreases. As shown in **Figure 3.8** and **Figure 3.9**, water saturation in these layers drops to zero before

100 days of production. For layer-4 of the fracture, water fills the fracture for a longer time compared to the upper layers. From plot in **Figure 3.10**, layer-4 of the fracture does not contain water after ~100 days. Water in layer-5 of the fracture retained longer than the upper layers, as shown in **Figure 3.11**. Perforation is only completed in the uppermost layer may cause a delay of water cleanup for the lowermost layer. After 100 days of production, water saturation in layer-5 of the fracture is still high (S_w>0.9). The fracture is free of water after around 180 days of production.

From the plot in **Figure 3.7** until **Figure 3.11**, we can see at t=200 days, fracture is completely free of water. There is no production restriction due to water presence in the fracture after 200 days.

Water saturation in the matrix near the fracture keeps high. It is observed for the first 50 days, water saturation drops fast to ~0.5. But after 50 days of production, water saturation keeps at value ~0.5. Water near the tip of the fracture remains trapped due to high capillary pressure in the matrix. It is accumulated in the matrix near the fracture. It will not be produced until the capillary pressure barrier is overcome. Very low matrix permeability is another reason the water remained in the matrix.

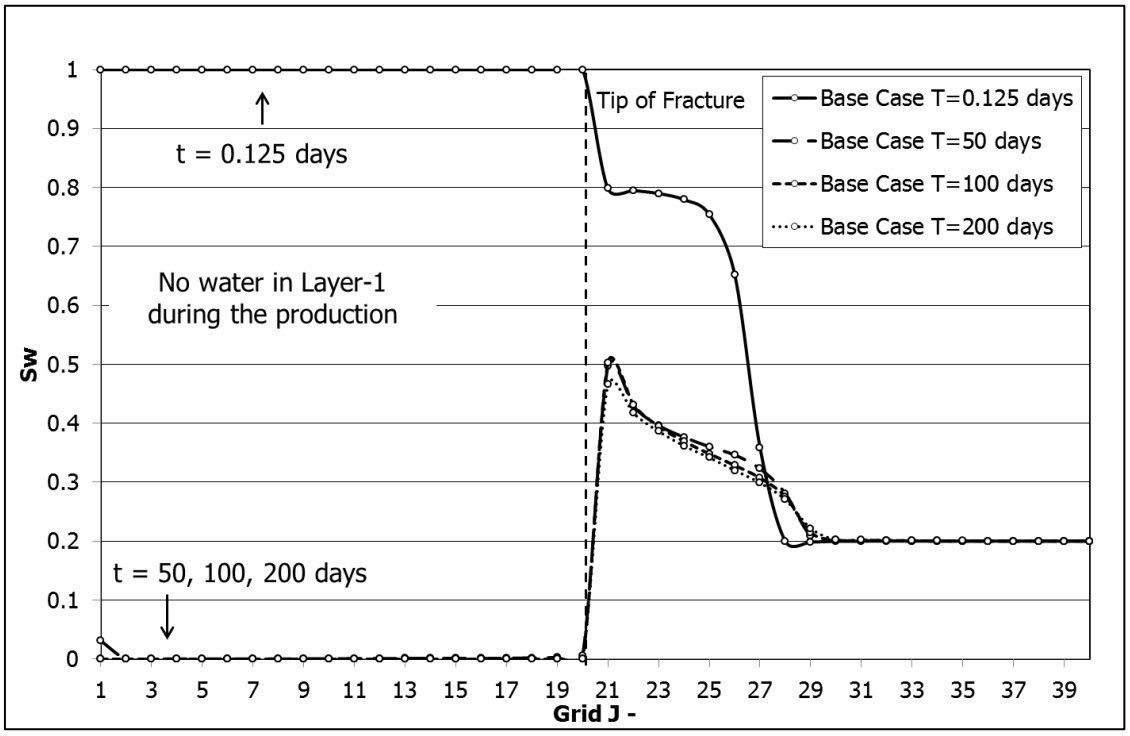

Figure 3. 7 – Base Case: Water Saturation Profile in Layer-1 (JK-cross section, I=15)

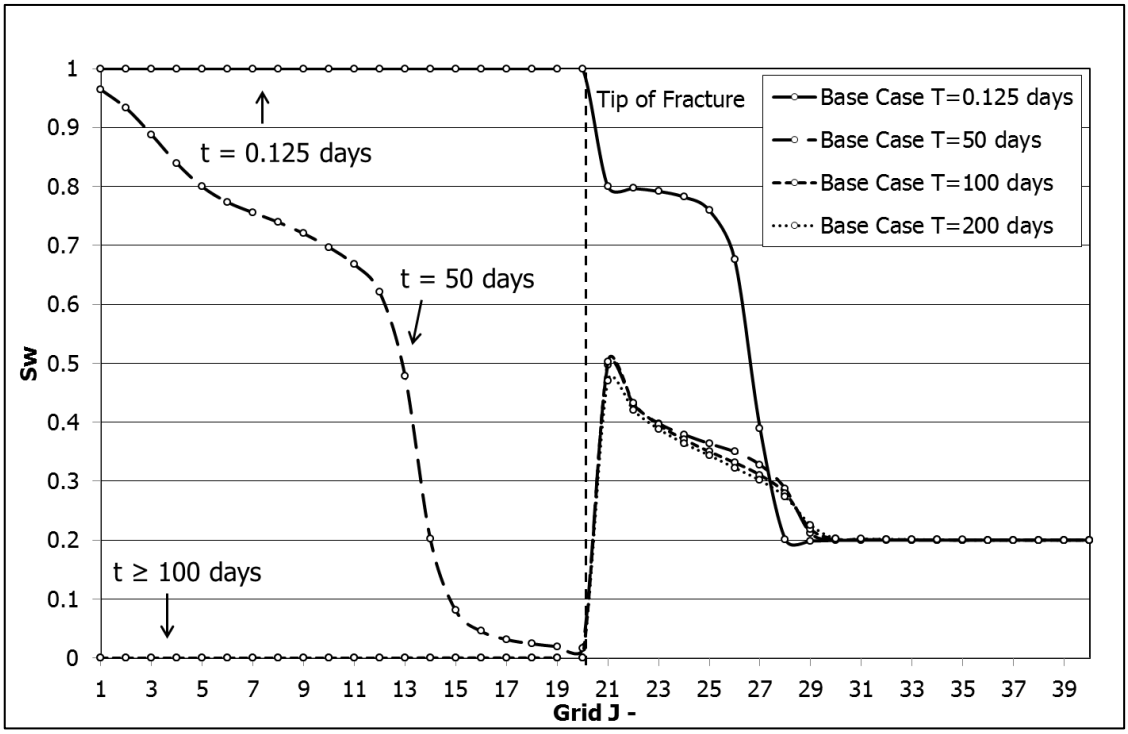

Figure 3. 8 – Base Case: Water Saturation Profile in Layer-2 (JK-cross section, I=15)

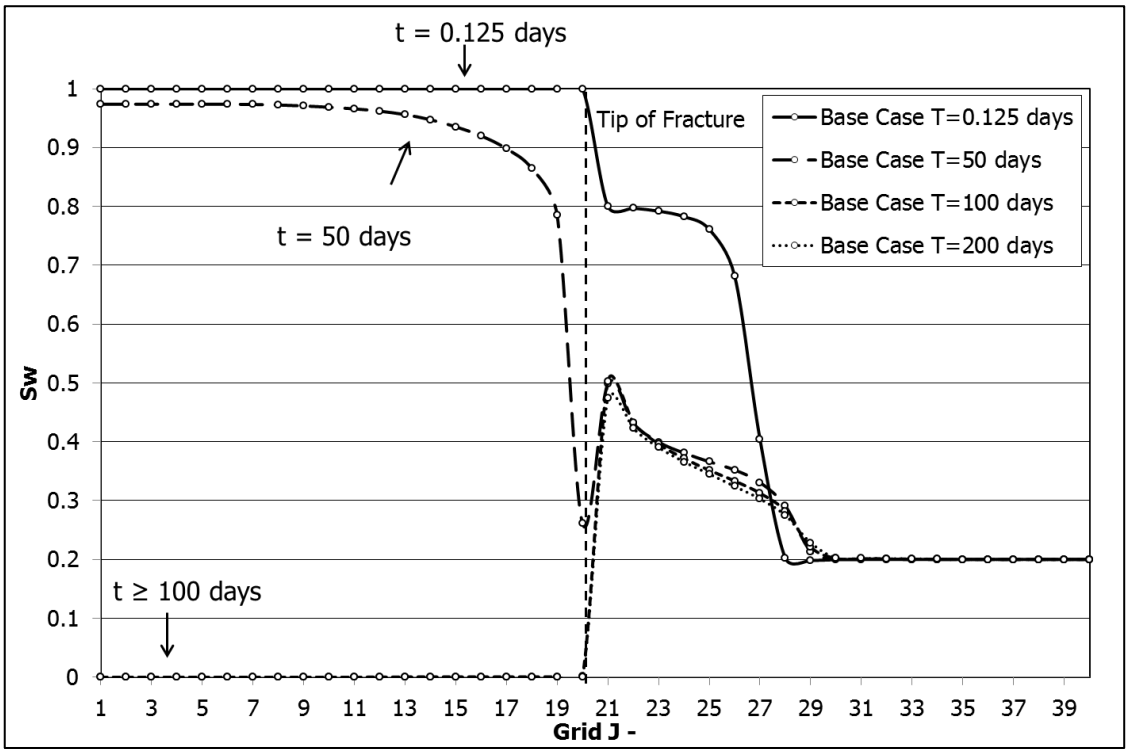

Figure 3. 9 – Base Case: Water Saturation Profile in Layer-3 (JK-cross section, I=15)

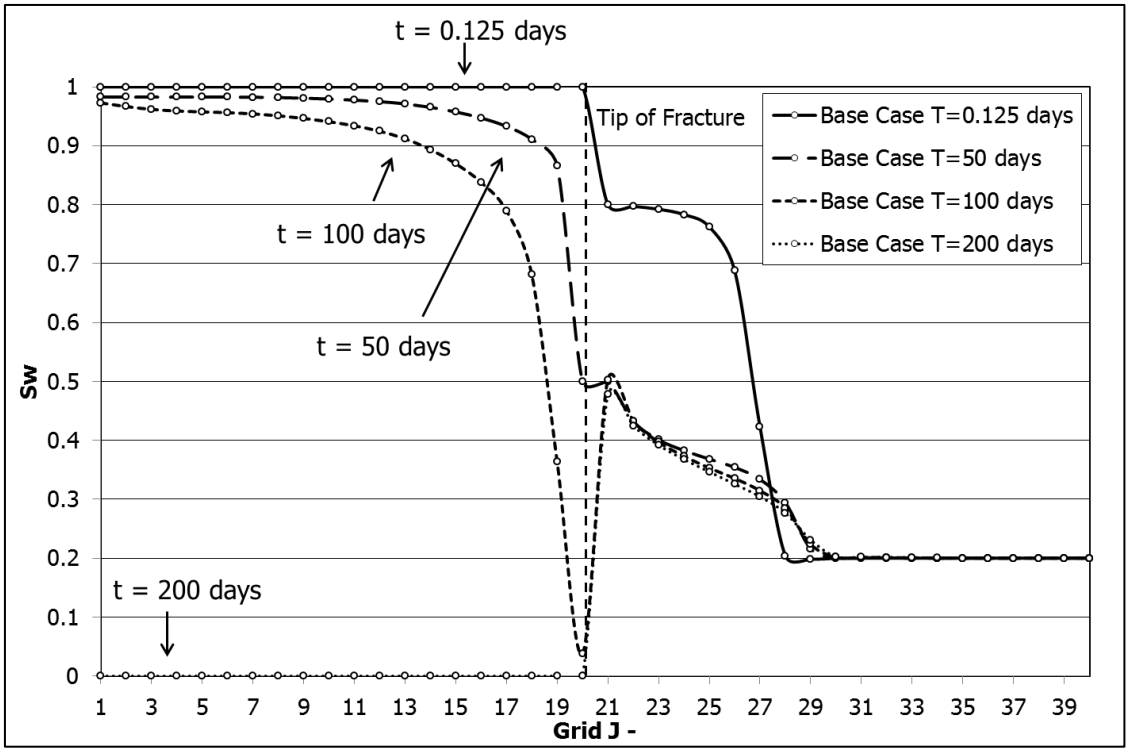

Figure 3. 10 – Base Case: Water Saturation Profile in Layer-4 (JK-cross section, I=15)

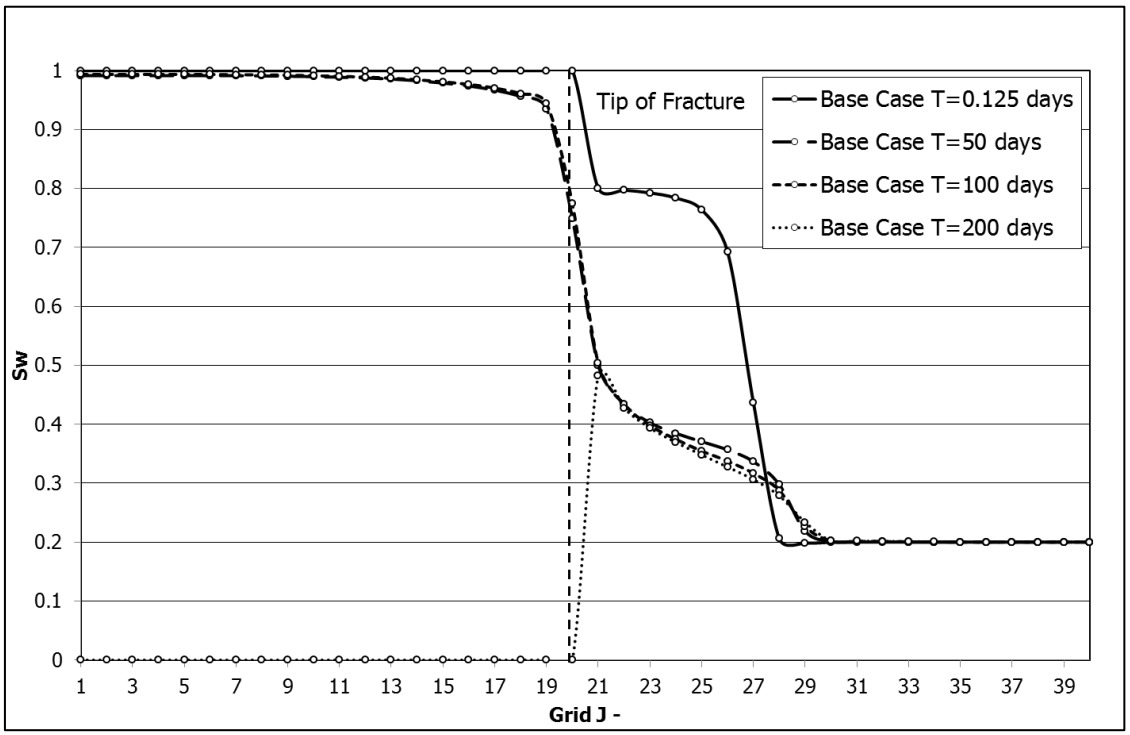

Figure 3. 11 – Base Case: Water Saturation Profile in Layer-5 (JK-cross section, I=15)

3.1.2 Production Profile

Figure 3.12 shows the bottomhole pressure and cumulative water injection per half fracture during water injection. To accommodate the safety factor during water injection, injection bottomhole pressure was set below the maximum injection bottomhole pressure. This injection condition is controlled by *m* values. The study shows that higher *m* value results in higher injection pressure.

Production constrain for the first 10 days after water injection was applied. For the first 10 days, water production was limited at 2,000 STB/d for one well (10 fractures). Commonly, water treatment capacity in the field is limited. Therefore, it was taken as a representation of production in the field. After 10 days, constrain of production was changed to constant bottomhole pressure. It was produced with constant bottomhole pressure 1500 psi.

Figure 3.13 shows the gas production profiles of the base case model. The gas production does not have plateau period. The cumulative gas production for 200 production days is 34.83 MMScf for a half-fracture. The initial gas in place for a half-fracture model is 1,498 MMScf. So that recovery factor is only 2.325%. For well production, it equals twice the half-model production time the total number of fractures.

The plot in **Figure 3.14** shows the water production profile for the base case. Total water production for the well reaches zero after ~57 production days. Water recovery until 200 production days is 0.5541 MSTB. Compared to 2,000 STB injected water, it indicates 27.7% of injected water is recovered to the surface.

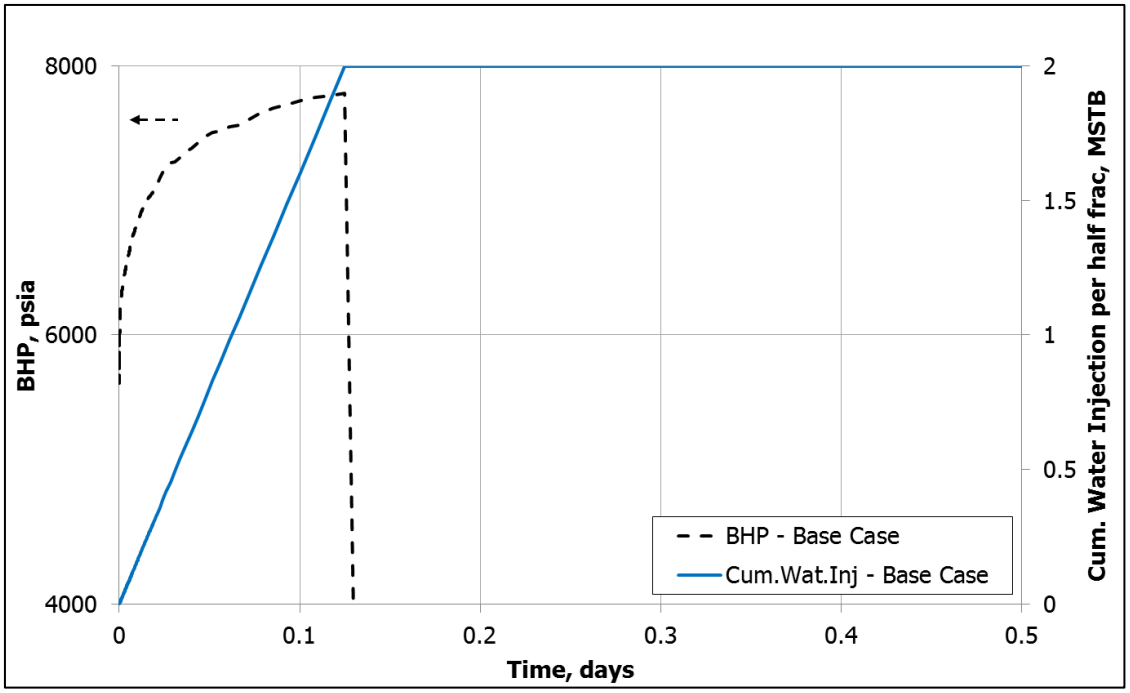

Figure 3. 12 – Base Case Model: Cumulative Water Injection per half fracture and Injection Bottomhole Pressure

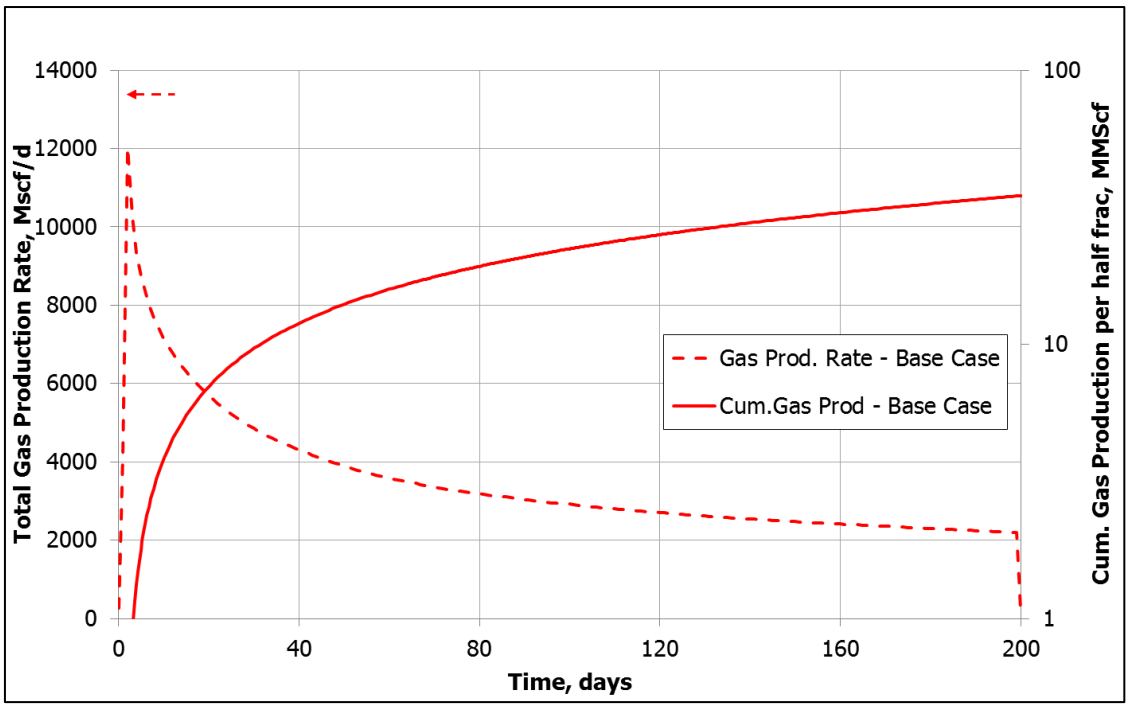

Figure 3. 13 – Base Case Model: Gas Production Profile

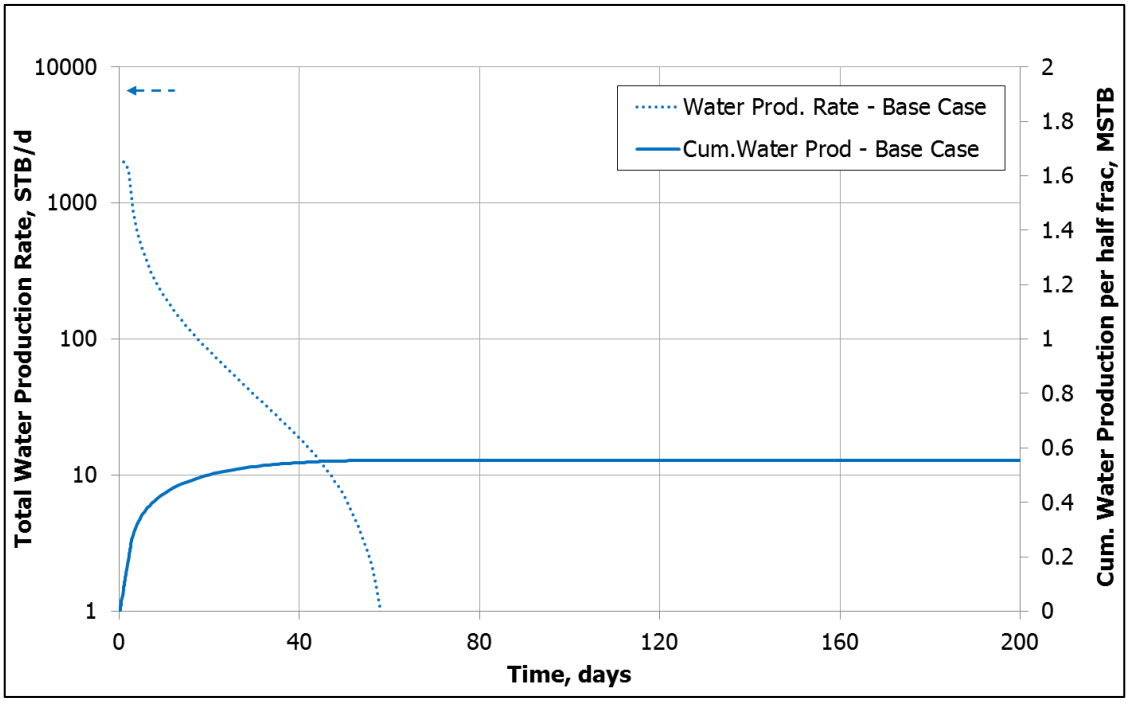

Figure 3. 14 – Base Case Model: Water Production Profile

3.2 Number of Layer Sensitivity

The finite-difference, where the spatial segmentation of reservoir model is discretized into grid blocks, is one basic of reservoir simulation. The discretization error term, Δx^2, will be smaller when the smaller grid blocks used. The smaller discretization of the grid blocks, the more time needed to simulate the model. This sensitivity was performed to see the effect of layer numbers on production profile of the model. In this sensitivity, only number of discretization in z-direction was conducted.

The number of layer in z-direction (N_z) for this sensitivity was set to 1, 3, 5, 10, 20, 30, and 40. For the model with more than 6,000 grids, full license of Sensor was used. There is a limitation for Sensor6k. It only can run the model with the total of grids less than 6,000.

The production constrain for this sensitivity is the same constrain as the base case. The well was controlled by a maximum water production rate of 2,000 STB/d for the first 10 days. Afterward, it was switched to a constant bottomhole pressure of 1,500 psi with maximum gas rate of 10,000 Mscf/d.

Figure 3.15 shows the cumulative water injection per half fracture and injection bottomhole pressure. For one layer model, higher pressure to inject water is required to accommodate

200 ft thickness of the layer. For model with more than 3 layers, required injection pressure is relatively the same.

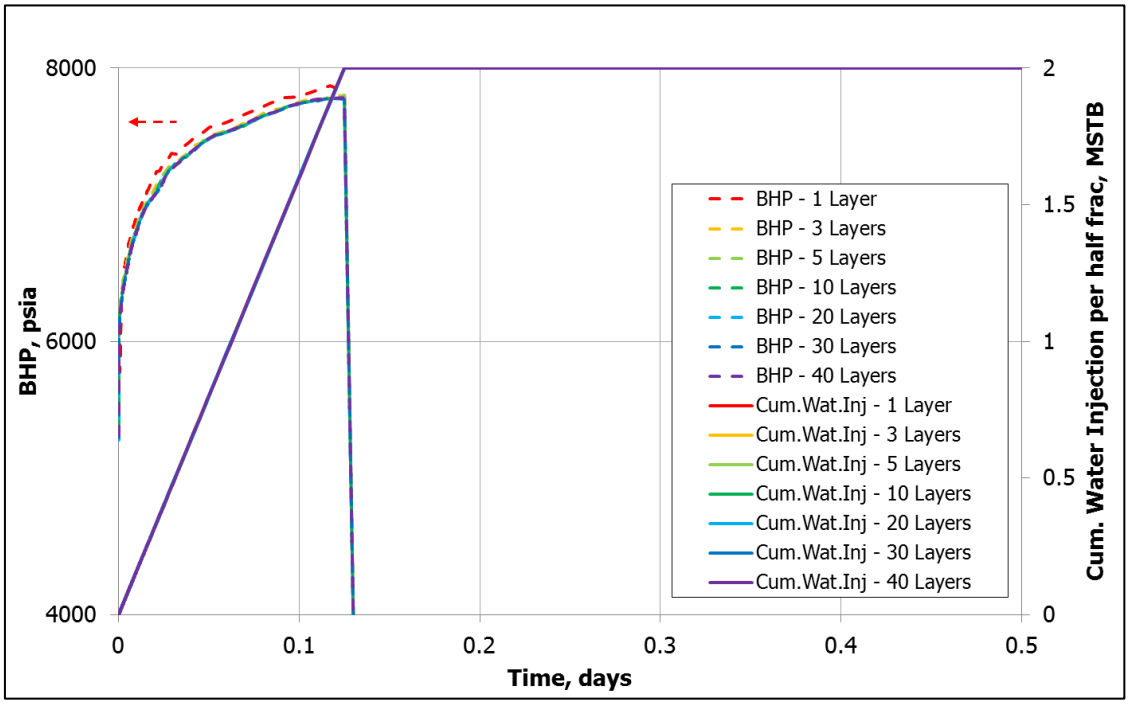

Figure 3. 15 – Sensitivity of Layer Number: Cumulative Water Injection per half fracture and Injection Bottomhole Pressure

For the gas production profile, one layer model gives higher initial gas rates compared to other model with higher layer numbers. **Figure 3.16** shows the differences of cumulative gas production for all cases are not significant. The conductivity in the fracture is so high that it does not make much difference if perforate is performed in a smaller thickness.

Water production profile can be seen in **Figure 3.17**. One layer model also gives longer water production time compared to other models. Consequently, cumulative water production for one layer model is also higher. For the case with higher layer numbers, water production rate profile is getting convergent. From the plot, it also shows the same convergence profile for cumulative water production. Five layers model for the study is then enough to represent cases with higher number of layers.

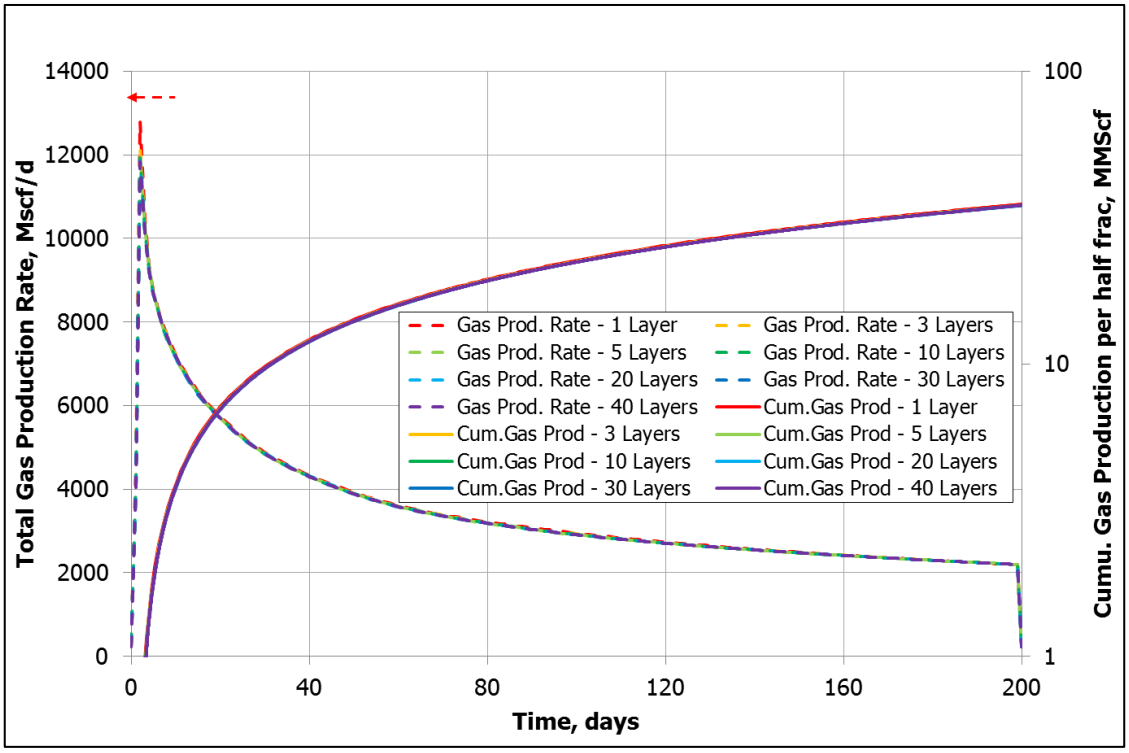

Figure 3. 16 – Sensitivity of Layer Number: Gas Production Profile

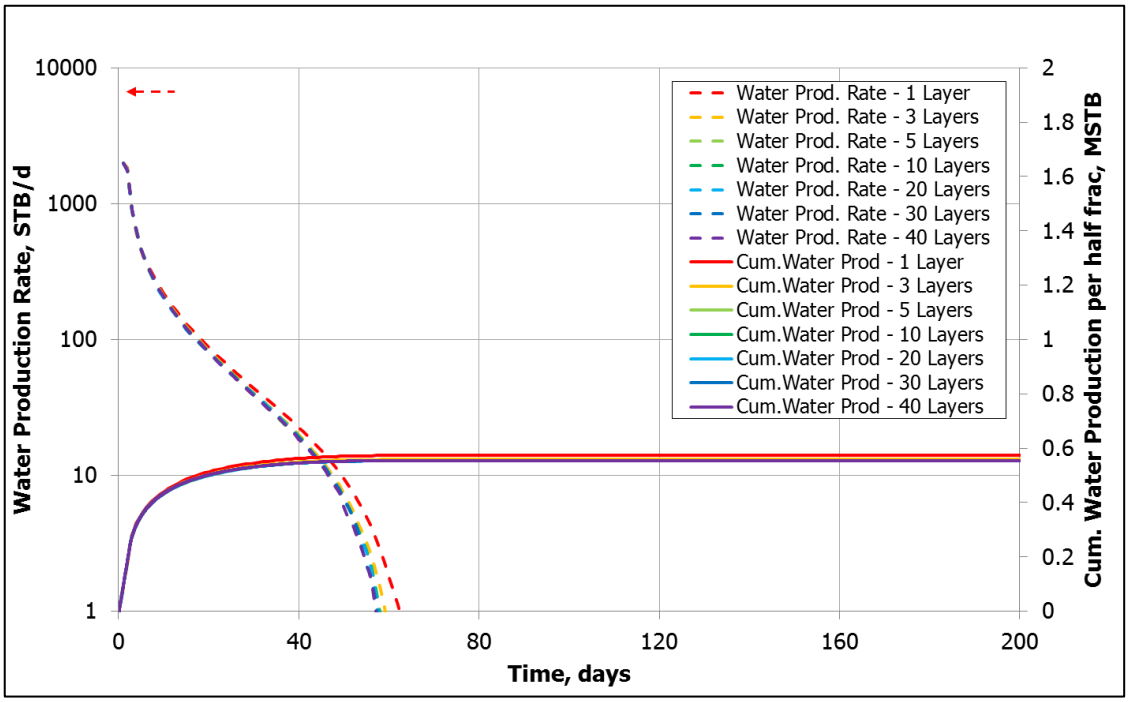

Figure 3. 17 – Sensitivity of Layer Number: Water Production Profile

3.3 Perforation Location Sensitivity

Sensitivity of perforation locations was performed to see the effect of different production point on production profile, especially water saturation in the fracture. Three different perforation locations was chose to see its effect. **Figure 3.18** shows different perforation locations; upper perforation at k=1, mid-perforation at k=3, and lower perforation at k=5.

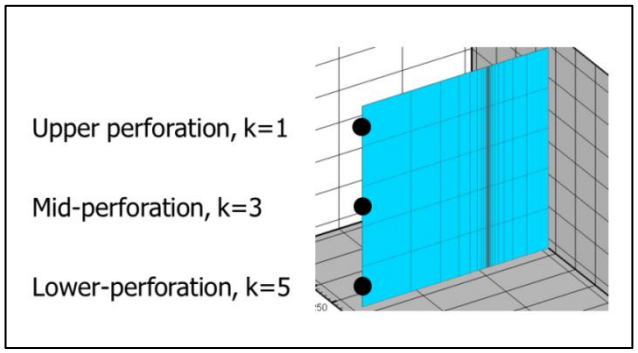

Figure 3. 18 – Sensitivity of Perforation Location

3.3.1 Water Saturation Profile

Water saturation profile in the fracture for each layer and different case can be seen in **Figure 3.19** until **Figure 3.23**. For all cases and all layers after water injection (t=0.125 days), fracture is filled with water (S_w=1). At the end of simulation (t=200 days), water saturation equals zero for all cases and for different layers.

As shown in Plot **Figure 3.19**, layer-1 of the fracture for all cases does not contain water during the production. There is a little amount of water, S_w=0.03, in grid J=1 for upper perforation case. But it becomes zero afterwards. Instantaneous water production, water imbibition into the formation, and water segregation due to gravity force are the reasons water saturation in layer-1 is zero.

Water saturation for mid-perforation case and lower perforation case is observed decreasing fast in layer-2 of the fracture, as shown in **Figure 3.20**. Perforated layer for these cases is located below layer-2, so that water saturation becomes zero before 50 production days. For the upper perforation case, water saturation needs more time to decrease. For this case at t=50 days, water saturation is observed still high near the perforation area. The water saturation in layer-2 of the fracture increases from the tip of the fracture (J=20, K=2) to the area near perforation (J=1, K=2) at t=50 days. After 100 production days, both for this case and other cases, layer-2 of the fracture is observed free of water.

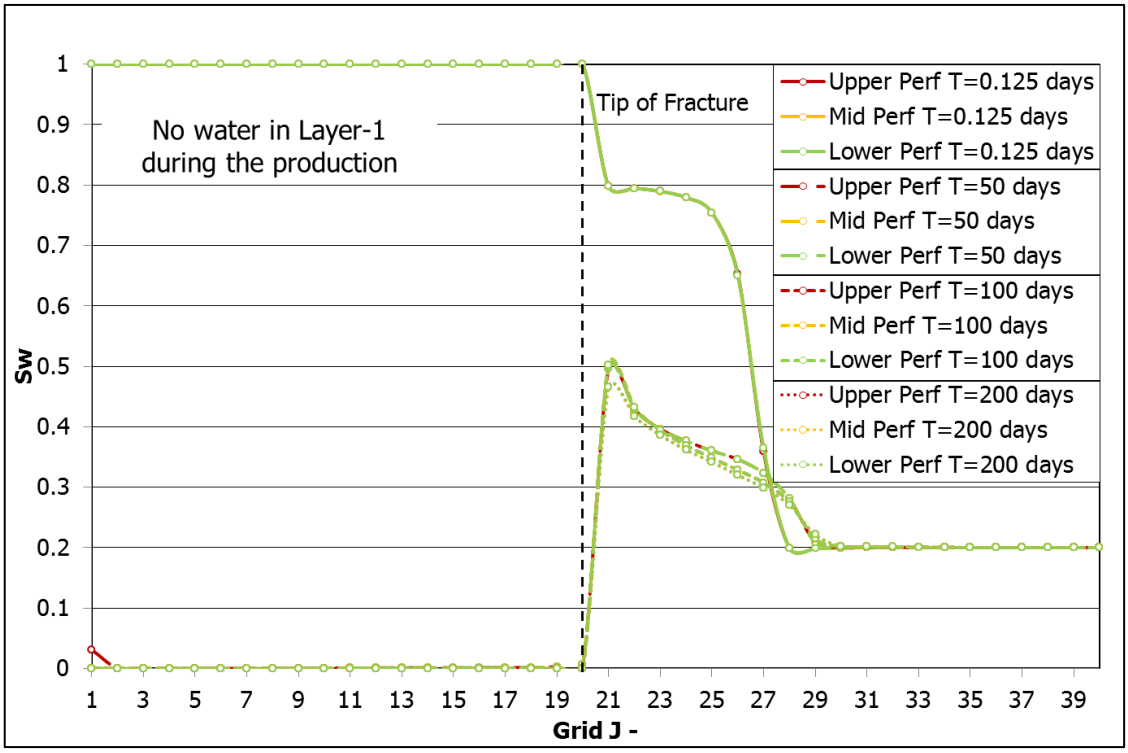

Figure 3. 19 – Sensitivity of Perforation Location: Water Saturation Profile in Layer-1 (JK-cross section, I=15)

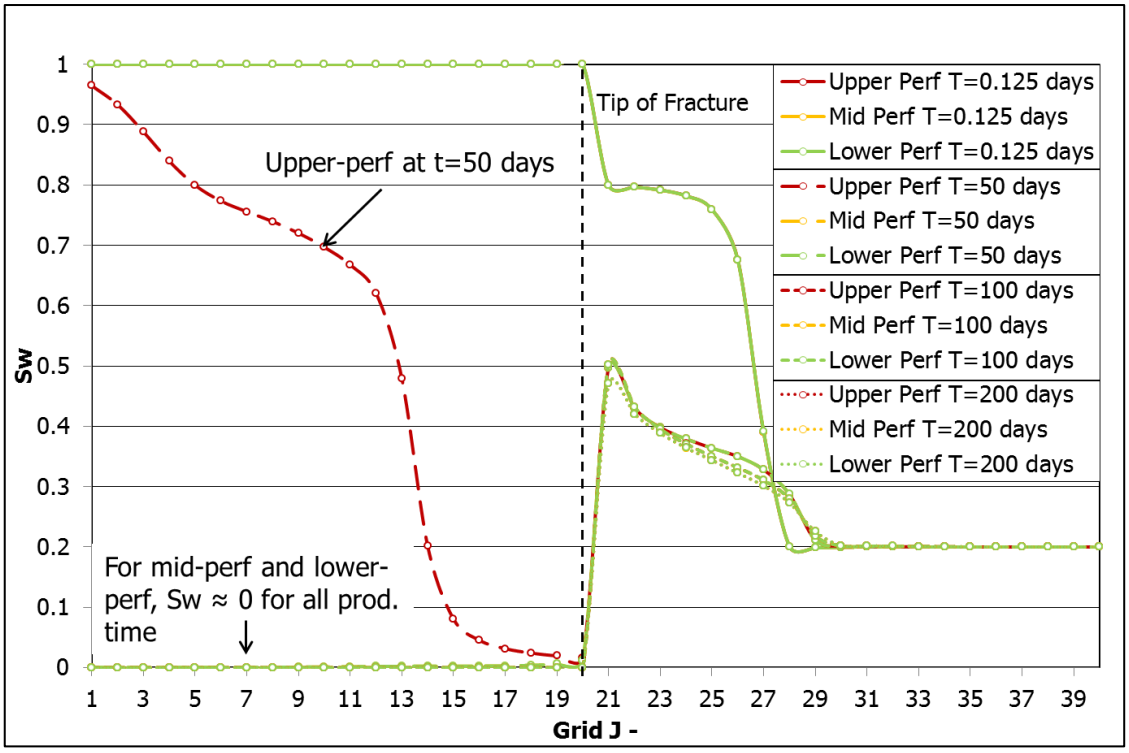

Figure 3. 20 – Sensitivity of Perforation Location: Water Saturation Profile in Layer-2 (JK-cross section, I=15)

As shown in **Figure 3.21,** water saturation in layer-3 of the fracture for mid-perforation case and lower perforation case is observed decreasing to zero by the time production started. A little amount of water (S_w=0.035) in grid J=1 at 50 days for mid-perforation case is also observed. Layer-3 is the layer where the perforation for mid-perforation case is located. So that water on that grid is still observed. Water from the lower layer is drawn to the perforation. The water saturation also drops to zero afterwards.

For lower perforation case, perforation is located on the lowermost layer. For this case, water in the fracture is produced through the lowermost layer. Gravity force also makes the water in the fracture to be easily produced. As a result, the water saturation in layer-3 for lower perforation case drops to zero during production. For upper perforation case, it is observed the water saturation is still high at t=50 days. Then, it decrease to zero with production, as observed at t=100 days.

Water saturation for lower perforation case in layer-4 of the fracture equals zero during the production, as shown in **Figure 3.22**. On the other hand, water is still observed at t=50 days and t=100 days for upper perforation case and mid-perforation case. For mid-perforation case, water saturation at 100 days is only observed at J=1. Decreasing in water saturation at layer-4 of the fracture for upper perforation case is observed slower compared to other cases. At t=100 days, water saturation is still high. For upper perforation case, perforation is located on the uppermost layer and it is far from layer-4. It results in delay water cleanup for the lower layers of the fracture.

The lowermost layer, which is layer-5, is the perforated layer for lower-perforation case. As shown in **Figure 3.23** for upper perforation and mid-perforation case, water saturation at t=50 days is as high as water saturation at t=100 days. It means water stays longer in this layer which is far from the perforation. Water is also observed in layer-5 of the fracture for lower perforation case. For this case at t=50 days, water saturation increases from the tip of the fracture (J=20) to the middle area of the fracture (J=10), then it decreases until J=1. It means the water is sucked down into the perforation layer.

The same profile is also observed at t=100 days for lower perforation case. For this case at t=100 days, it is likely that re-imbibition of water into the matrix is occurred. Since the water saturation near the perforation grid (J=1 until J=7) is zero, but for grid J>7 is observed higher than zero. For lower perforation case, water accumulation is not observed in almost all layers. Water tends to be more easily produced to the wellbore due to perforation in the lowermost zone.

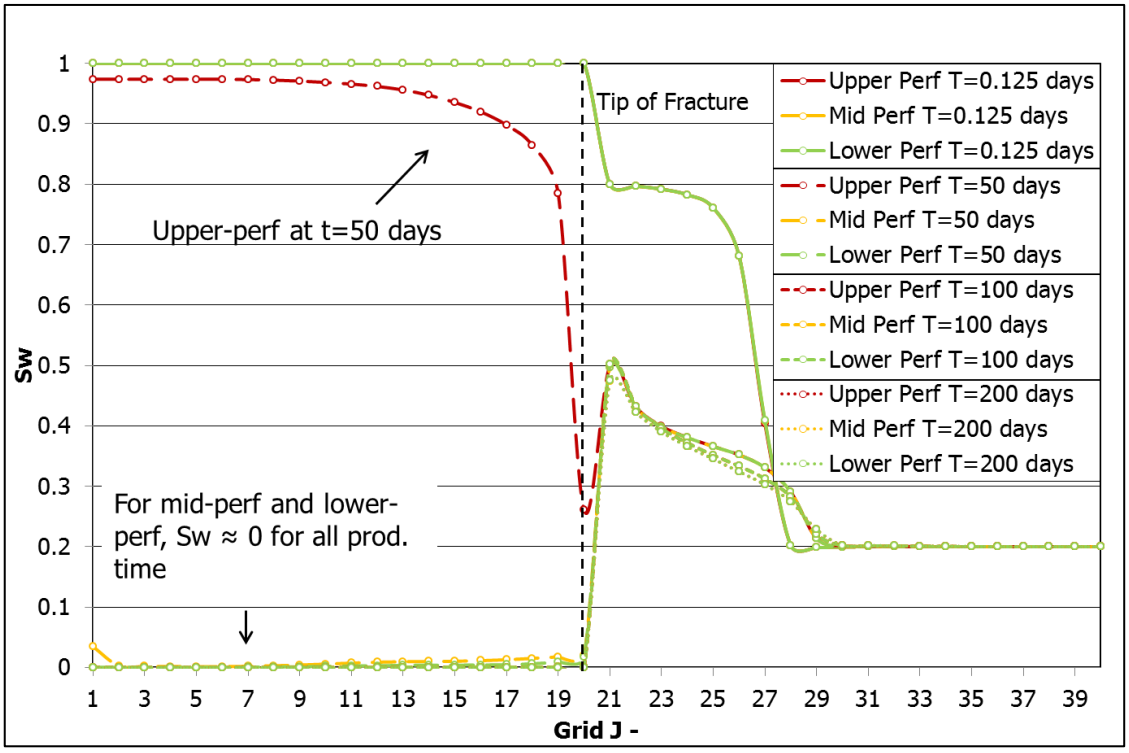

Figure 3. 21 – Sensitivity of Perforation Location: Water Saturation Profile in Layer-3 (JK-cross section, I=15)

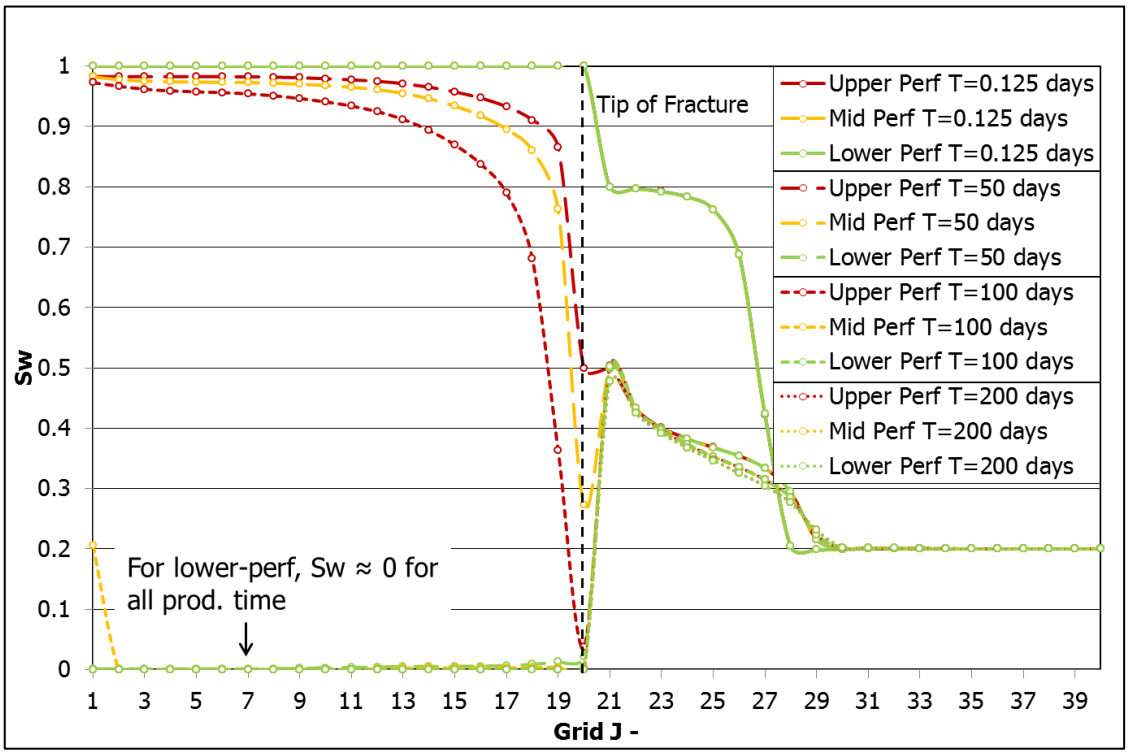

Figure 3. 22 – Sensitivity of Perforation Location: Water Saturation Profile in Layer-4 (JK-cross section, I=15)

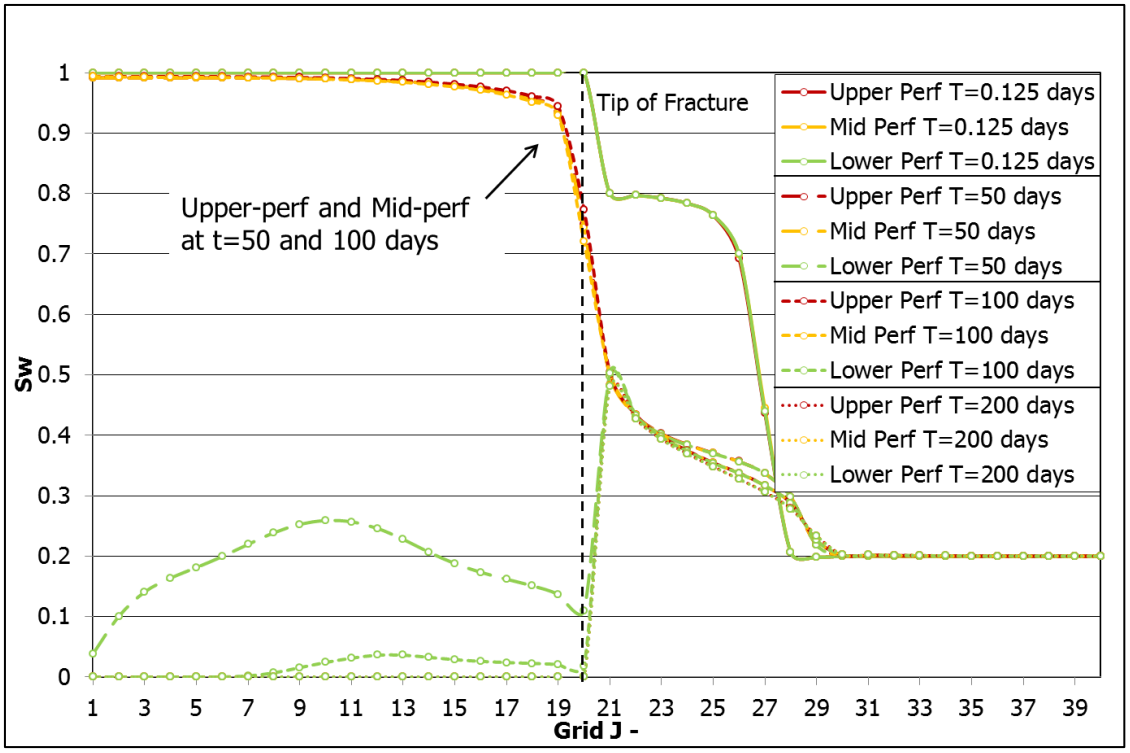

Figure 3. 23 – Sensitivity of Perforation Location: Water Saturation Profile in Layer-5 (JK-cross section, I=15)

3.3.2 Production Profile

The plot in **Figure 3.24** shows the cumulative water injection per half fracture and injection bottomhole Pressure. For the same amount of injected water, higher pressure is needed to inject water for lower perforation case. Different 40 ft in depth of perforation between different cases is the reason. When the perforation is moved upward, required injection pressure decreases.

Gas production profile for different cases can be seen in **Figure 3.25**. Gas production is less affected by different perforation location. For a half fracture model, gas recovery is 34.98 MMscf (RF=2.336%) for mid-perforation case, while for lower perforation is 35.09 MMscf (RF=2.343%). The upper perforation case gives 34.83 MMscf in gas recovery (RF=2.325%). Different amount of recovered gas shows that water presence in the fracture has impact on the gas flow. For example: the lower perforation case has less water in the fracture, therefore the gas flow has less restriction compared to other cases with higher water saturation in the fracture. But the overall gas production profile insignificantly affected by different perforation locations.

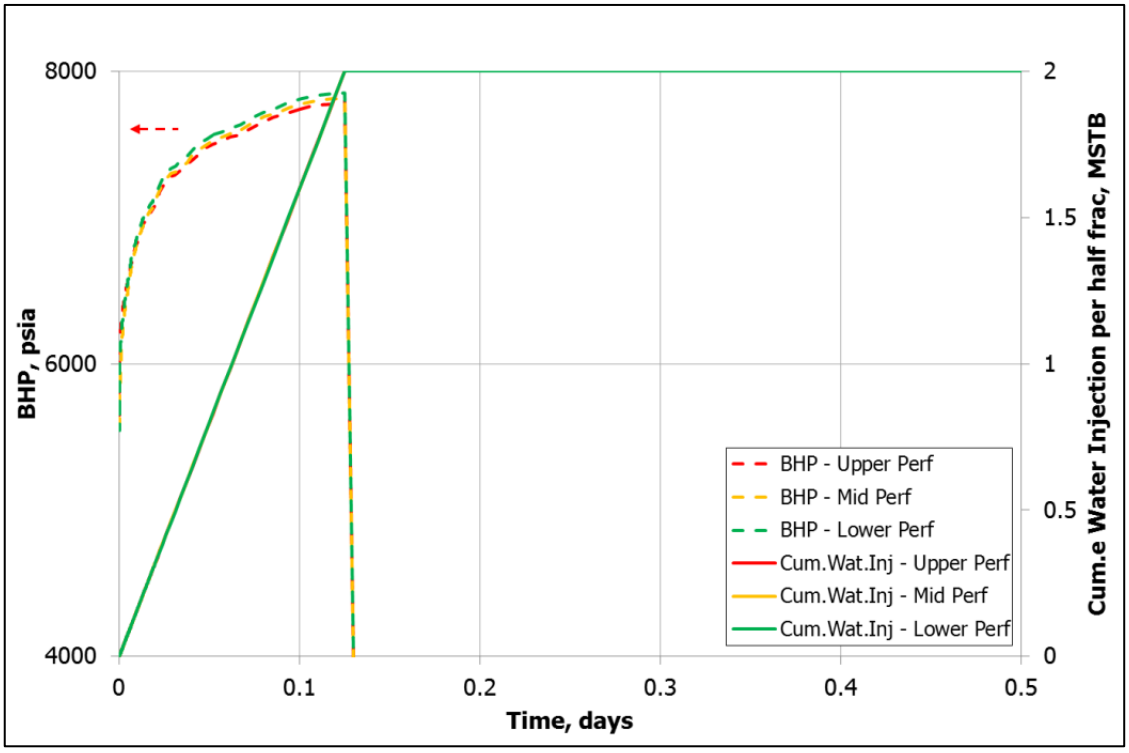

Figure 3. 24 – Sensitivity of Perforation Location: Cumulative Water Injection per half fracture and Injection Bottomhole Pressure

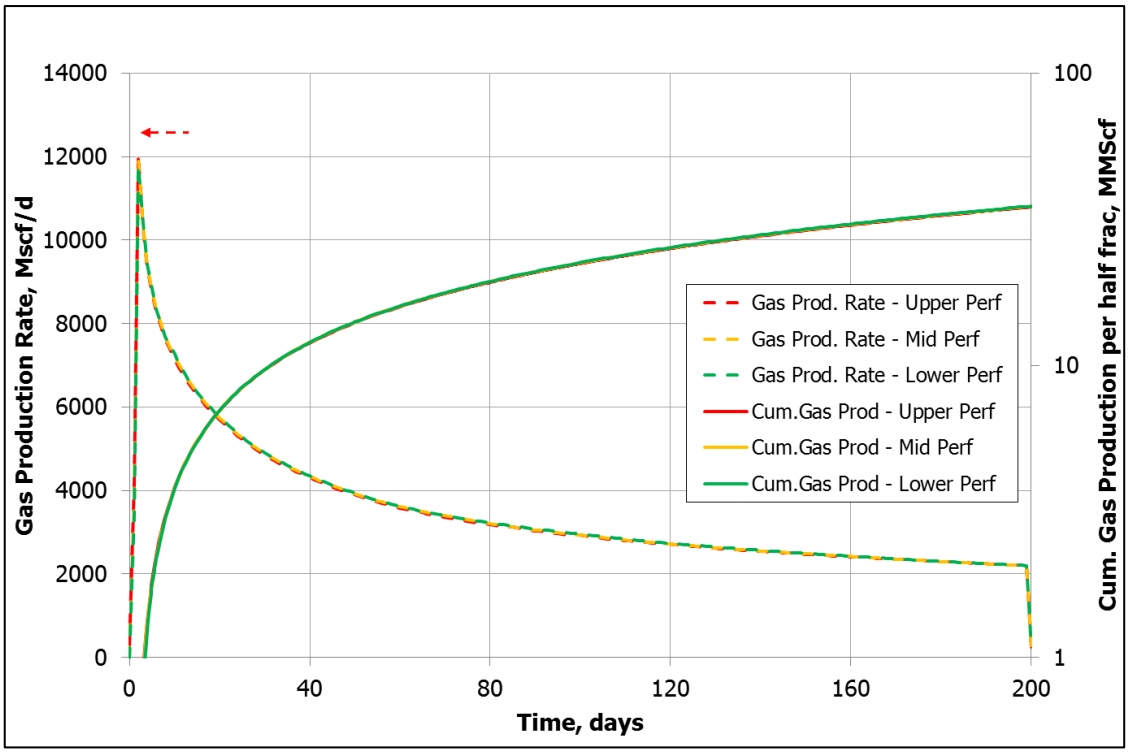

Figure 3. 25 – Sensitivity of Perforation Location: Gas Production Profile

Plot in **Figure 3.26** shows water production profile. For the same production constraint, lower perforation case gives longer water production yet slightly higher in gas production. According to water saturation analysis, water in lower perforation case is easier to recover due to perforation location at the lowermost of formation. The cumulative water production of half-fracture model for this case is 0.5772 MSTB or 28.8% of injected water is recovered. For the mid-perforation case is 0.567 MSTB or 28.3%, while for the upper perforation case results in water recovery 0.5441 MSTB or 27.7%.

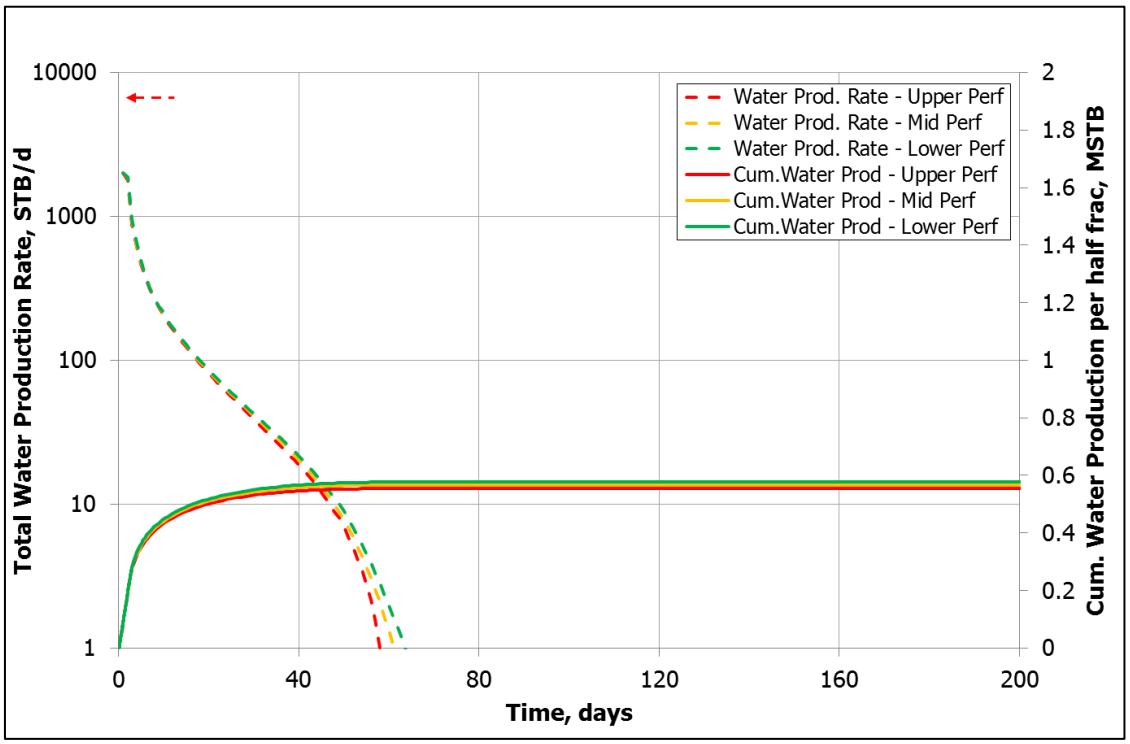

Figure 3. 26 – Sensitivity of Perforation Location: Water Production Profile

3.4 Permeability Sensitivity

To get a better understanding of the effect heterogeneity between layers, sensitivity of matrix permeability was conducted. The effect of the heterogeneity on the distribution of water saturation in the fracture itself was observed. In this permeability sensitivity, two different cases have been run. The first case is a case with the matrix permeability value decreasing downward. It means the lowermost layer has the lowest permeability. In this analysis, it is called 'decreasing matrix permeability case'. The second case is a case with the matrix

permeability value increasing downward, which means the highest permeability is in the lowermost layer. For this case, it is called 'increasing matrix permeability case'.

The base case has the same properties for all layers, which is 0.0002 mD in permeability and 10% in porosity. For the permeability sensitivity, the total *kh* (transmissibility) for the model is maintained at a constant. So that the total *kh* for both cases is the same, as stated in **Equation 3.6**. Permeability values that have been used in the permeability sensitivities are shown in **Table 3.4**.

$$\bar{k} \sum_{j=1}^{n} h_j = \sum_{j=1}^{n} k_j h_j \qquad (3.6)$$

Table 3. 4 – Permeability Value for Permeability Decreasing Downward Case and Permeability Increasing Downward Case

Permeability Decreasing Downward		
h (ft)	**k (md)**	**Porosity**
40	0.00034759	0.1
40	0.00025573	0.1
40	0.00018116	0.1
40	0.00012552	0.1
40	0.00009	0.1

Permeability Increasing Downward		
h (ft)	**k (md)**	**Porosity**
40	0.00009	0.1
40	0.00012552	0.1
40	0.00018116	0.1
40	0.00025573	0.1
40	0.00034759	0.1

3.4.1 Water Saturation Profile

Water saturation profiles for permeability sensitivity can be seen from **Figure 3.27** to **Figure 3.31**. After 0.125 days or 3 hours water injection, fracture is filled with water (S_w=1). From the plot, it also can be seen if the fracture is free of water at t=200 days for all cases.

For layer-1 of the fracture in the plot **Figure 3.27**, no water presence is observed in the fracture during production. Water in this layer is produced by the time well is opened. Water also segregates during production and imbibes into the matrix formation.

As shown in **Figure 3.28** during the first 50 production days, water saturation for all cases in layer-2 of the fracture increases from the tip of the fracture (J=20) to near the wellbore (J=1). The decreasing matrix permeability case gives the highest water saturation profile. It shows that water in the upper layer is more mobile due to higher matrix permeability than other cases. Consequently, matrix with higher permeability, for e.g. layer-1 and layer-2, will feed water to the fracture easier. Water saturation for this layer decreases along with production and it is observed to be zero for t>100 days.

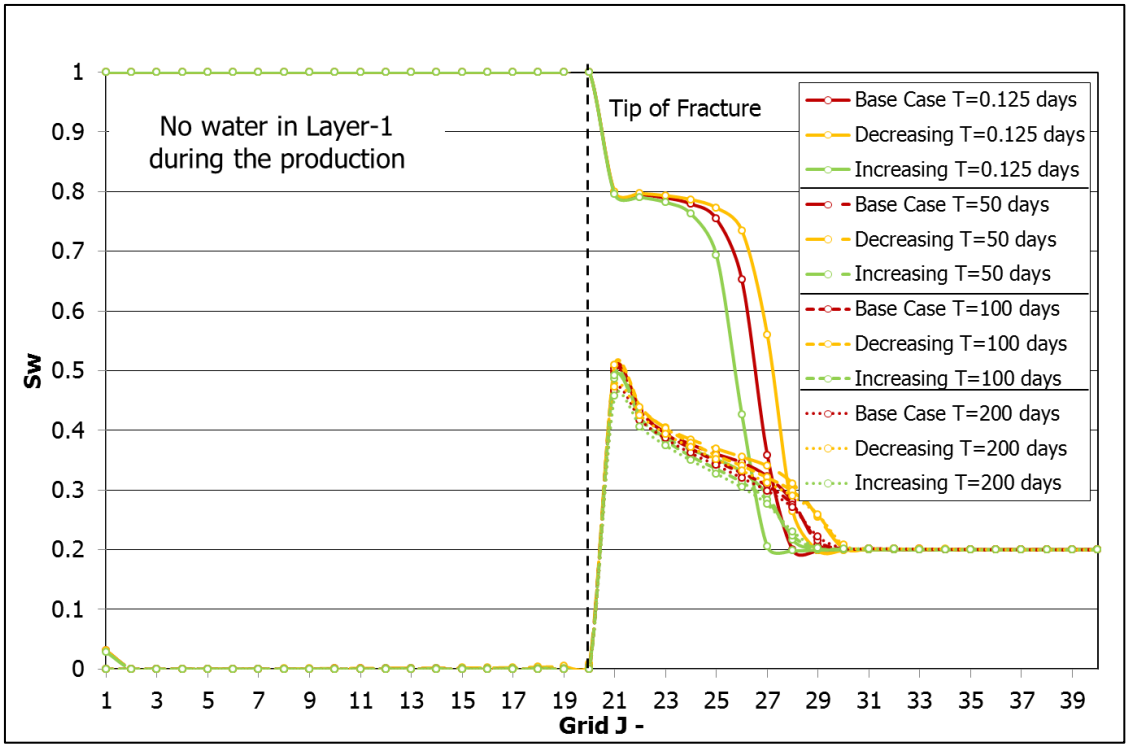

Figure 3. 27 – Sensitivity of Permeability: Water Saturation Profile in Layer-1 (JK-cross section, I=15)

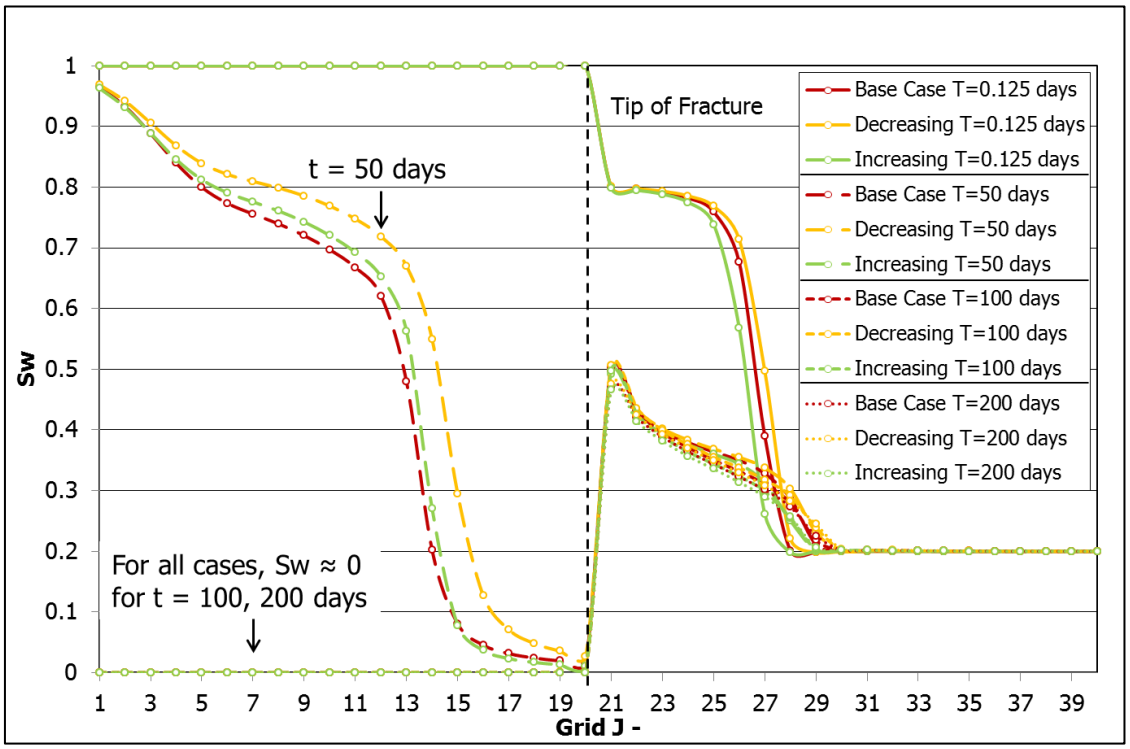

Figure 3. 28 – Sensitivity of Permeability: Water Saturation Profile in Layer-2 (JK-cross section, I=15)

Water saturation in layer-3 of the fracture at t=50 days, as shown in the plot **Figure 3.29**, is high for all cases. It is observed at t=50 days, decreasing matrix permeability case gives the highest water saturation if compared to both increasing matrix permeability case and base case. At t=100 days, water saturation in the fracture is zero for both base case and increasing permeability case, except for decreasing permeability case. Water saturation at t=100 days for decreasing permeability case is still high at J=1 and J=2. Higher amount of water influx due to higher matrix permeability in the upper layer may cause water saturation for decreasing matrix permeability case is higher than other cases.

At layer-4 of the fracture, water saturation at t=50 days for all cases is higher than the water saturation in the upper layer. Water saturation for increasing matrix permeability case decreases faster from t=50 days to t=100 days than other cases as shown in **Figure 3.30**. For increasing matrix permeability case, water saturation in this layer decreases faster due to low water saturation in the upper layer. So that water in the fracture from matrix layer-4 is produced due to less water influx from the upper layer. Therefore, water saturation in the fracture for increasing matrix permeability case decreases faster in this layer.

In layer-4 of the fracture, it is observed water saturation for decreasing matrix permeability case is still high at t=50 days and t=100 days. Water in the lower fracture zone is not lifted to the perforation layer because of more water influx from the upper layer. Thus, water stays longer in this layer.

From the plot in **Figure 3.31**, water saturation in layer-5 of the fracture is still high (S_w>0.9) for all cases until 100 days of production. Water stays longer in the lowermost layer than the upper layers. Perforation, is located in the uppermost layer, is far from layer-5 and it delays water cleanup for this layer.

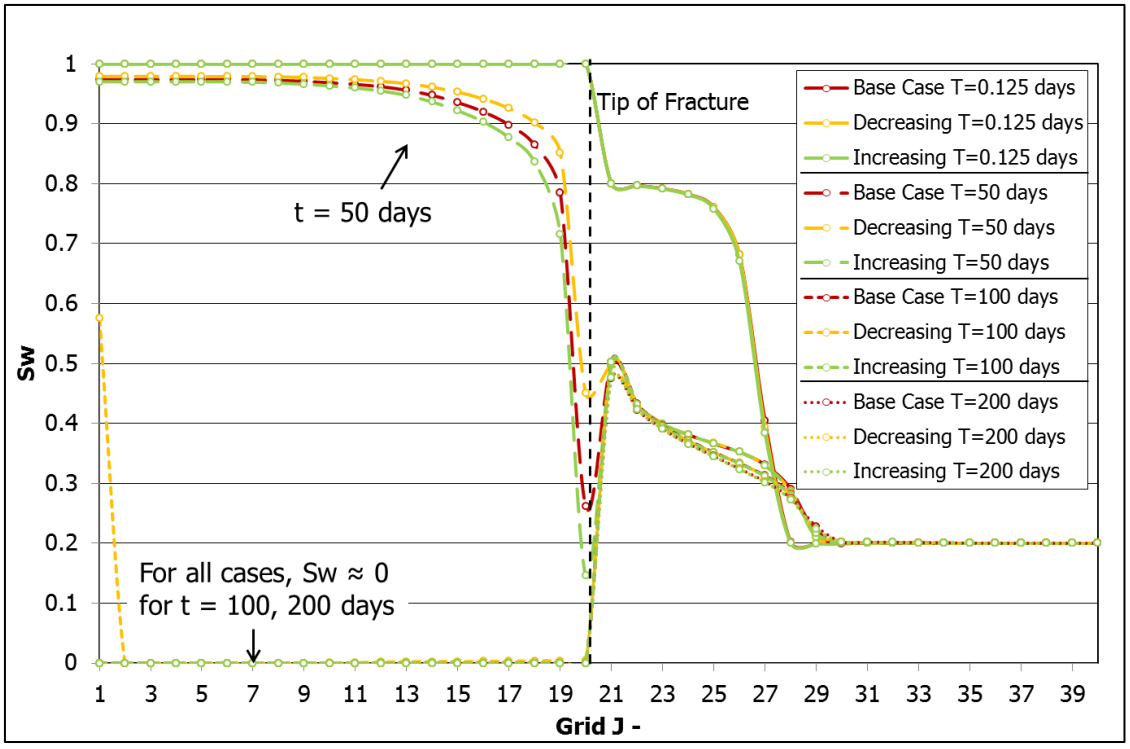

Figure 3. 29 – Sensitivity of Permeability: Water Saturation Profile in Layer-3 (JK-cross section, I=15)

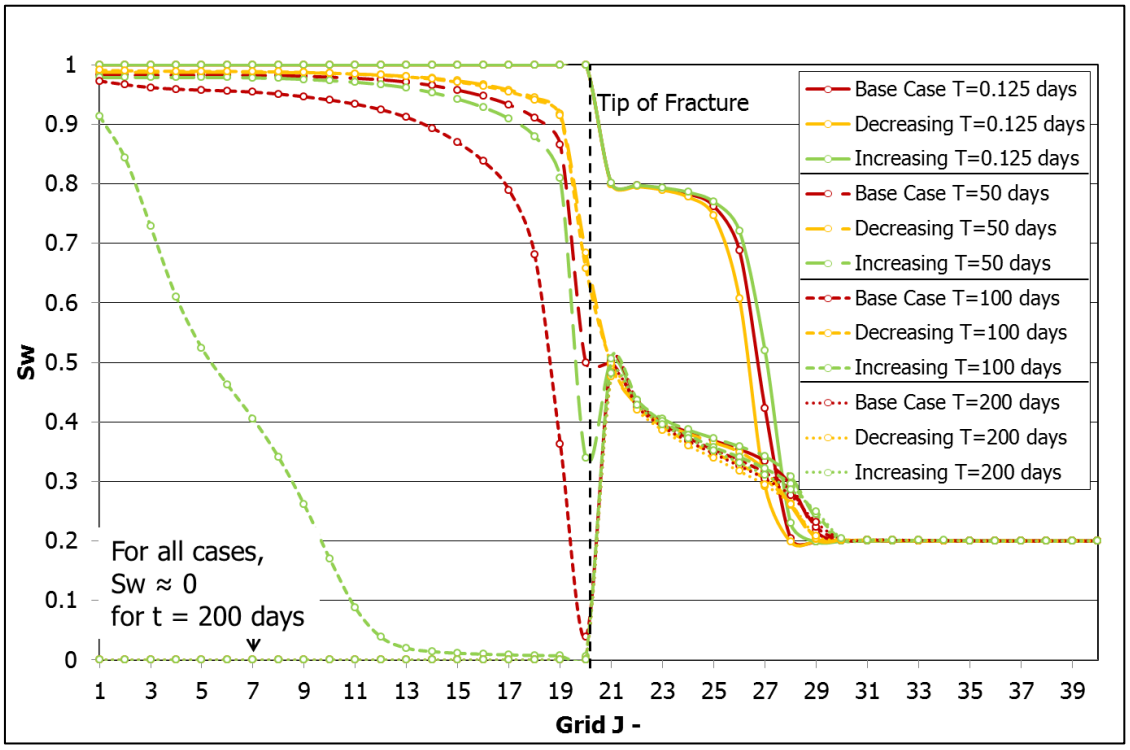

Figure 3. 30 – Sensitivity of Permeability: Water Saturation Profile in Layer-4 (JK-cross section, I=15)

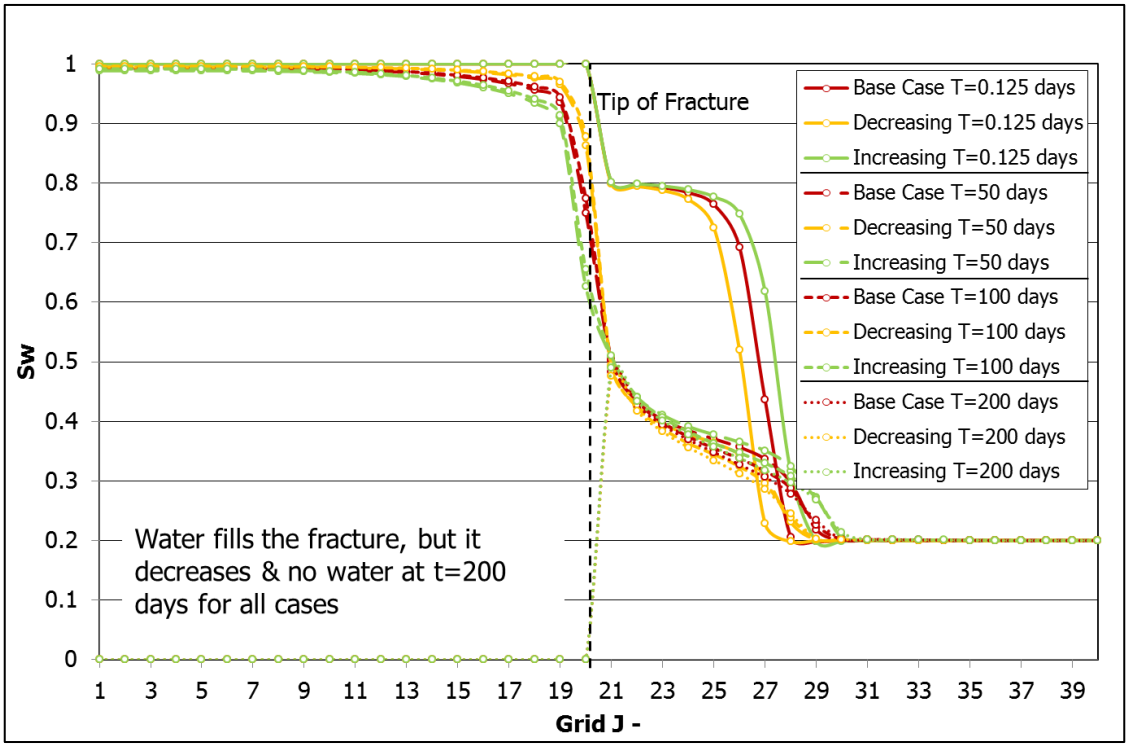

Figure 3. 31 – Sensitivity of Permeability: Water Saturation Profile in Layer-5 (JK-cross section, I=15)

3.4.2 Production Profile

Figure 3.32 shows the cumulative water injection per half fracture and injection bottomhole pressure. For all cases, required injection pressure is relatively the same. Different matrix permeability for different layers has insignificant effect for the required water injection pressure. The same total of *kh* for all cases could be the reason.

Gas production profile can be seen in **Figure 3.33**. The base case profile has slightly higher rate than two other case. The lowest gas rate profile is given by the matrix permeability increasing case. But overall, different permeability in the matrix has insignificant effect on gas production profile for different cases, as long as the model has the same total of *kh*. For the base case, gas recovery is 2.345%. The decreasing permeability case gives 2.262% in gas recovery, while the increasing permeability case gives 2.258%. As observed in water saturation analysis, the increasing matrix permeability case has the lowest water saturation compared to other case at the same observed time. But it does not result in the largest gas recovery, on the other hand it gives the lowest gas recovery. For the increasing matrix permeability case, high matrix permeability layer is located far from the perforated layer. Water saturation in the lowermost layer of fracture is observed high during the production, so that gas recovery is lower compared to other cases.

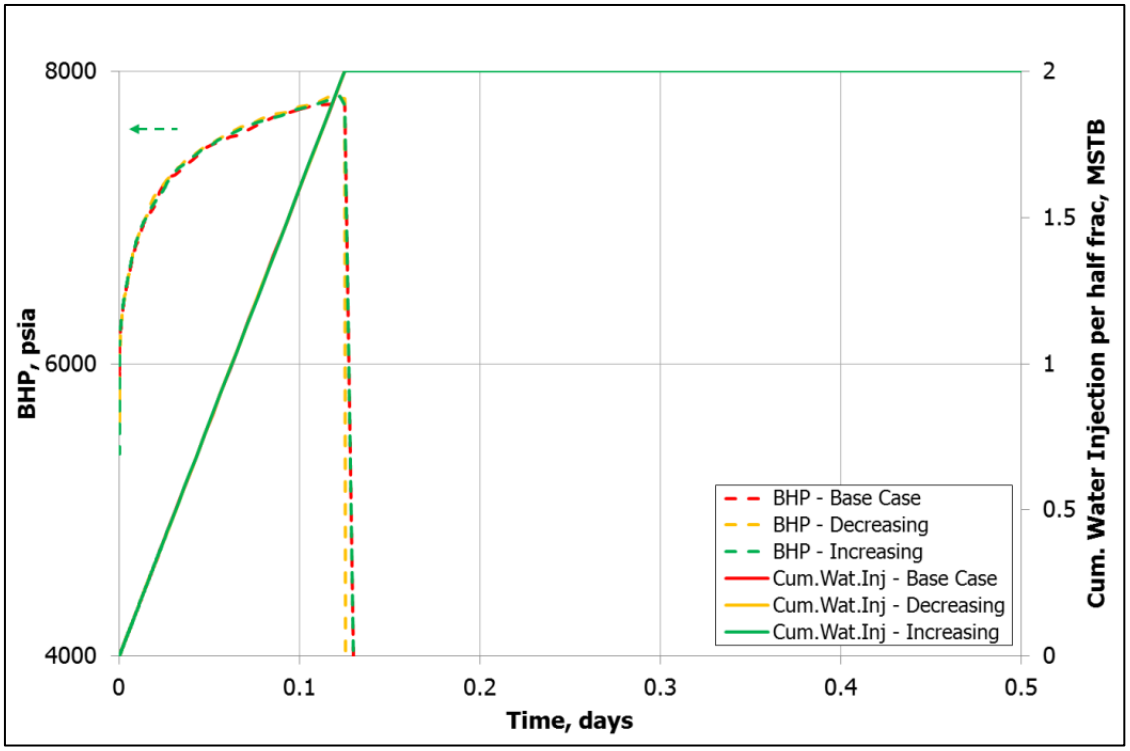

Figure 3. 32 – Sensitivity of Permeability: Cumulative Water Injection per half fracture and Injection Bottomhole Pressure

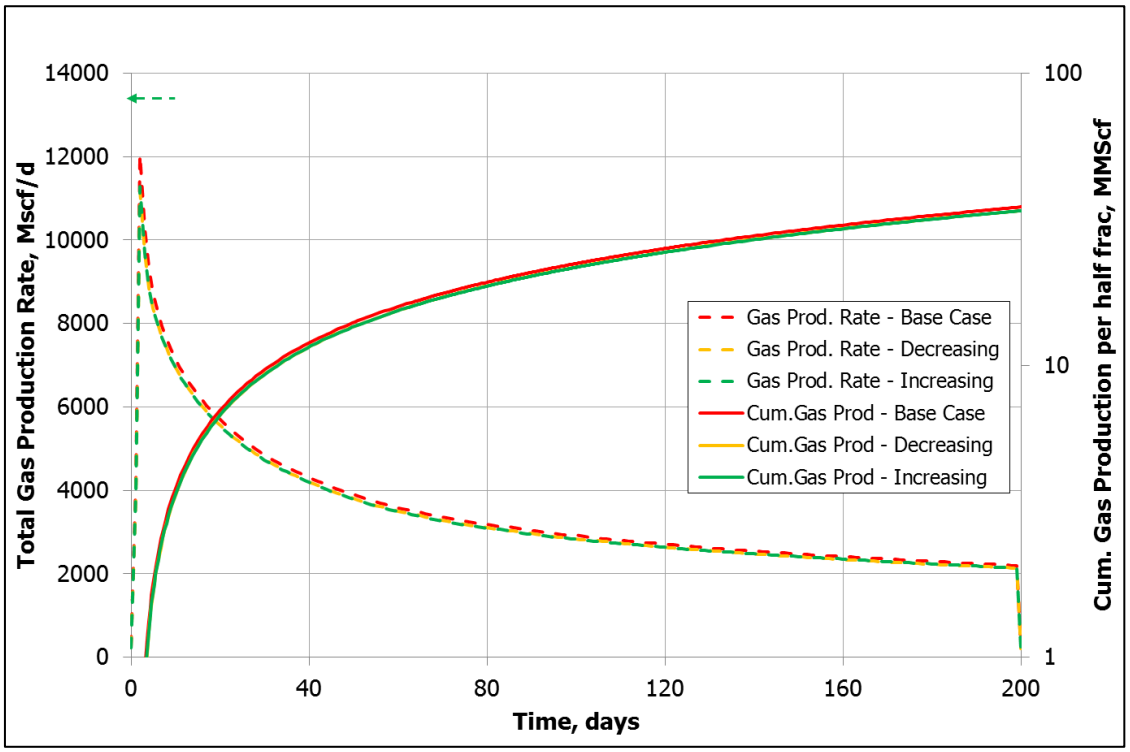

Figure 3. 33 – Sensitivity of Permeability: Gas Production Profile

Plot in **Figure 3.34** shows water production profile for matrix permeability sensitivity. The decreasing matrix permeability case gives slightly longer water production. The decreasing matrix permeability case has higher permeability around the perforated layer. Water cleanup is more effective when the perforated layer is around the high matrix permeability. Higher permeability in the upper matrix layer not only gives higher water recovery, but also higher gas recovery.

For the increasing matrix permeability case, high matrix permeability is located far from the perforation. Water from the lower zone is easier to flow to the fracture for this case but it is far from perforation, so that the water production rate is relatively lower compare to the decreasing permeability case. Cumulative water production of half-fracture model for the base case is 0.5541 MSTB (27.7%). For the decreasing permeability case, it indicates 0.5638 MSTB or 28.2% of injected water is recovered to the surface. The increasing permeability case results in 0.5585 MSTB water productions or 27.9% of injected water is recovered.

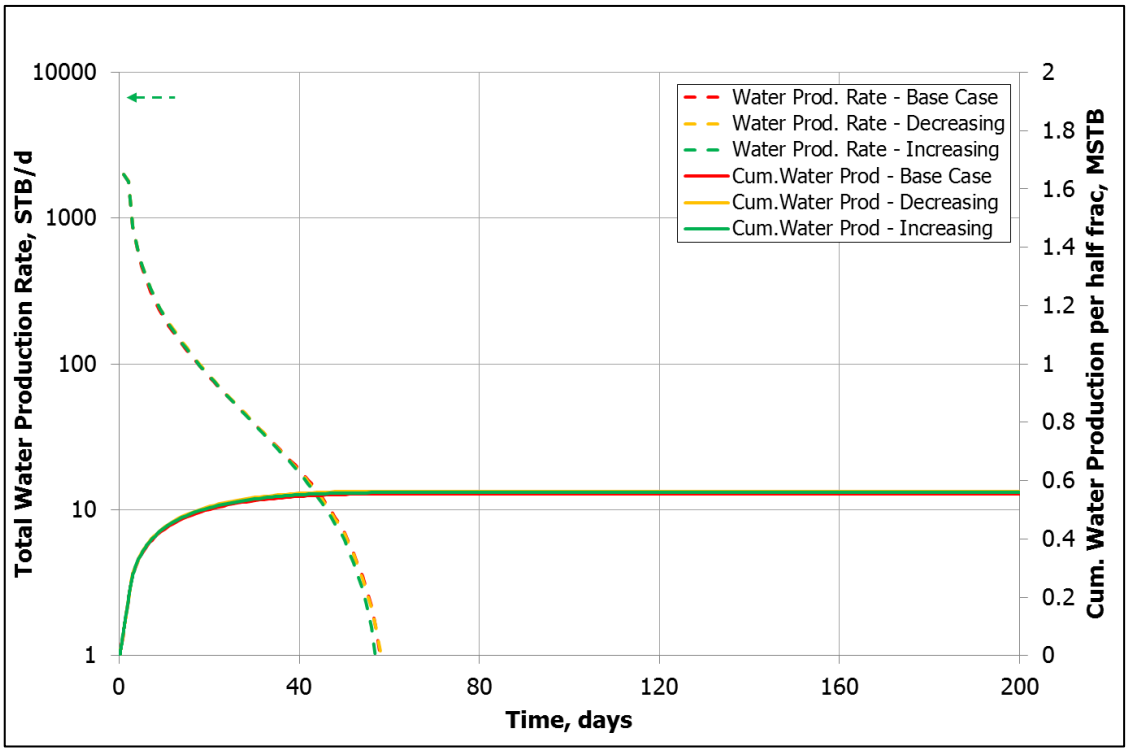

Figure 3. 34 – Sensitivity of Permeability: Water Production Profile

3.5 Rate Sensitivity

To see the effect of different gas rate on water saturation in the fracture, this sensitivity was performed. The rate from 500 Mscf/d until 10,000 Mscf/d was chose to see its effect on water behavior. There are two different cases for rate sensitivity. The first case, the production has water constrain for the first 10 days of production. The maximum water rate for the first 10 days is 2,000 STB/d. Then after 10 days, well is controlled by a constant bottomhole pressure. While for the second case, the production does not have water constrain. Only constant bottomhole pressure is applied for this case.

3.5.1 Rate Sensitivity with Water Constrain

3.5.1.1 Water Saturation Profile

Water saturation for rate sensitivity with water constrain can be seen from **Figure 3.35** to **Figure 3.39.** Fracture is filled with the water (S_w=1) after 3 hours water injection for all different rates and all layers. Water saturation equals zero is observed for all cases and all different layers at the end of simulation.

For layer-1 of the fracture, there is no water during production as shown in **Figure 3.35**. Water is instantaneously produced when production is commenced. Water also imbibes into the formation and also segregates during production until the end of simulation time.

Water saturation in layer-2 of the fracture for rate 500 until 2,000 Mscf/d is zero for all production time. After the production is started, water saturation in the fracture decreases faster than other rates. It can be seen in **Figure 3.36** for rate 5,000 Mscf/d and 10,000 Mscf/d, water saturation at t=50 days is high. Sufficient gas rate, which leads to drawdown pressure, may be needed to bring the water from the matrix to the fracture. Water in the fracture from the matrix re-imbibes to the formation for cases with rate below 2,000 Mscf/d.

Layer-3 of the fracture shows high water saturation for the case with gas rate 5,000 Mscf/d and 10,000 Mscf/d. At 50 days, water saturation for those two cases is similar. Water is still observed for gas rate 5,000 Mscf/d and 10,000 Mscf/d at t=100 days as shown in **Figure 3.37**. But for other gas production rates, water saturation decreases to zero along with the production, which can be seen at t=100 days and t=200 days.

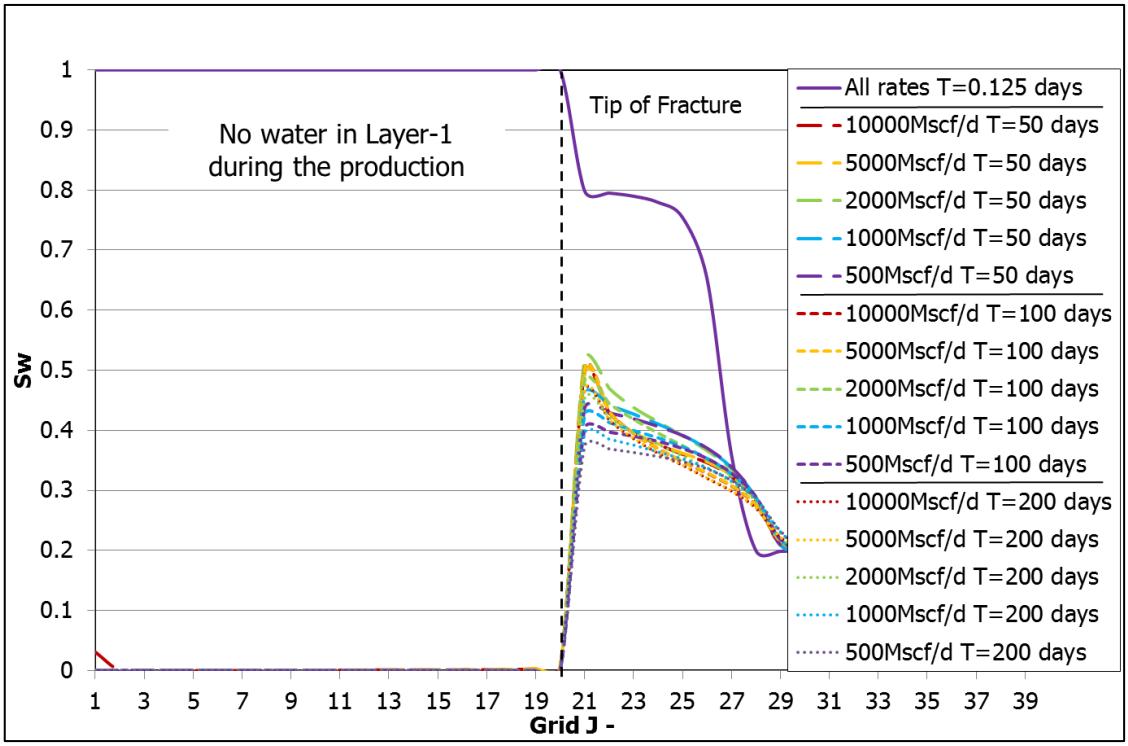

Figure 3. 35 – Sensitivity of Rate with Water Constrain in Layer-1: Water Saturation Profile (JK-cross section, I=15)

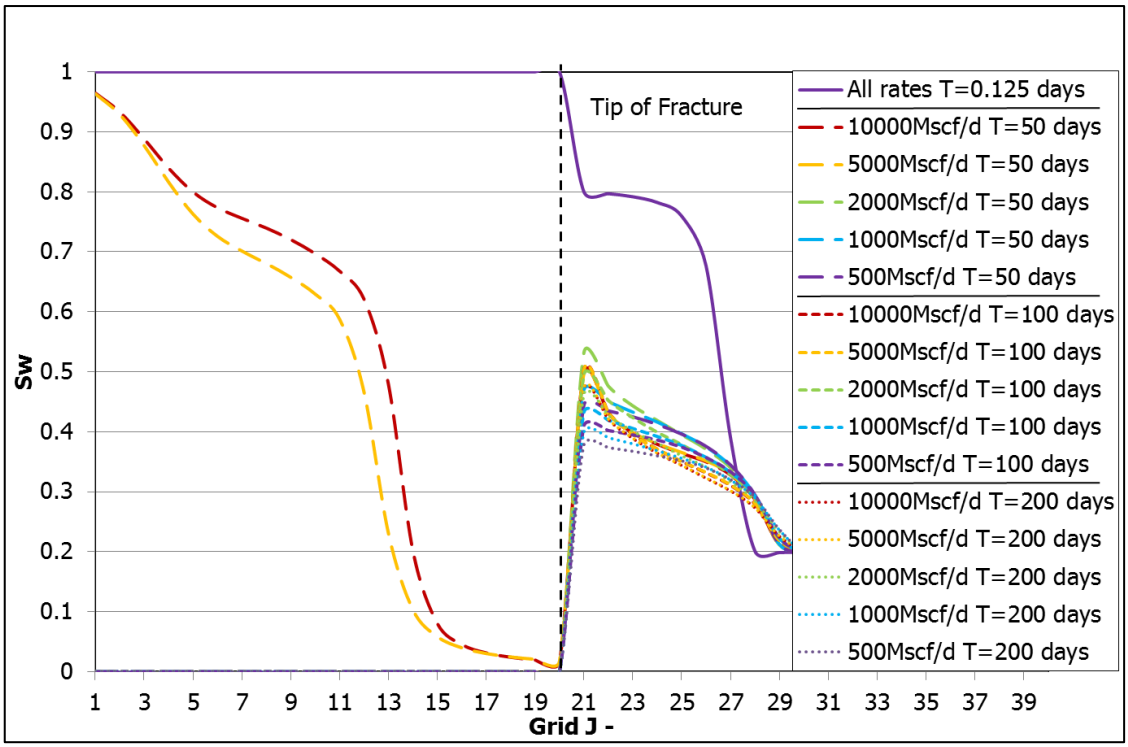

Figure 3. 36 – Sensitivity of Rate with Water Constrain in Layer-2: Water Saturation Profile (JK-cross section, I=15)

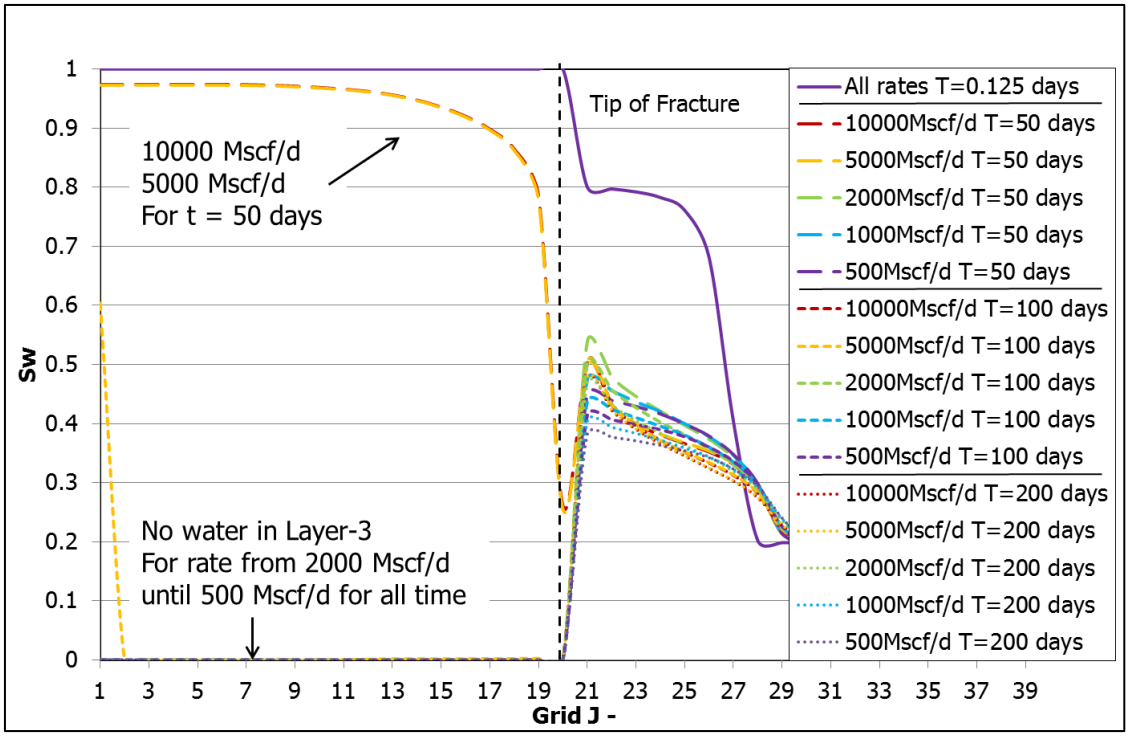

Figure 3. 37 – Sensitivity of Rate with Water Constrain in Layer-3: Water Saturation Profile (JK-cross section, I=15)

The same behavior is found for water saturation for layer-4 of the fracture for the gas rate 5,000 Mscf/d and 10,000 Mscf/d. Water saturation in layer-4 of the fracture at t=50 days is high for these two rate cases. It is also observed that water saturation for the case with gas rate 5,000 Mscf/d is higher than the case with gas rate 10,000 Mscf/d at t=100 days. High gas rate also lead to high water production. Therefore, water saturation for the case with gas rate 10,000 Mscf/d at t=100 days is observed lower as shown in Plot for Layer-4 in **Figure 3.38**.

High water saturation (S_w>0.9) for gas rate 5,000 Mscf/d and 10,000 Mscd/f is observed in layer-5 of the fracture. It is still observed that water stays in the fracture until 100 production days. Influx water from the matrix still feeds the fracture due to high gas rate.

As shown in **Figure 3.39**, water presence in layer-5 of the fracture is also observed for the case with gas rate 2,000 Mscf/d at t=100 days. It is expected that after water injection, water in the fracture is produced to the wellbore and some of it re-imbibes into the formation. For the gas rate 2,000 Mscf/d, water re-imbibes into the formation after water reaches the fracture. It can be seen at grid J=9 until J=15 for this rate at t=50 days. The water is sucked toward the perforation due to the drawdown, but the water does not reach the perforation

(J=1 and J=2). As we can see for the case with gas rate 2,000 Mscf/d in the upper layers, water is not observed for all times in the upper layers.

In layer-5 of the fracture, water saturation equals zero for the gas rate 500 Mscf/d and 1,000 Mscf/d. Water saturation in the matrix near the tip of the fracture decreases with production. But water saturation for these two cases is observed zero in the fracture. Water from the matrix reaches the fracture, but the gas rate is too low to produce the water, so that water may re-imbibe into the formation. At t=200 days for all cases, the fracture is free from the water since water saturation is observed zero.

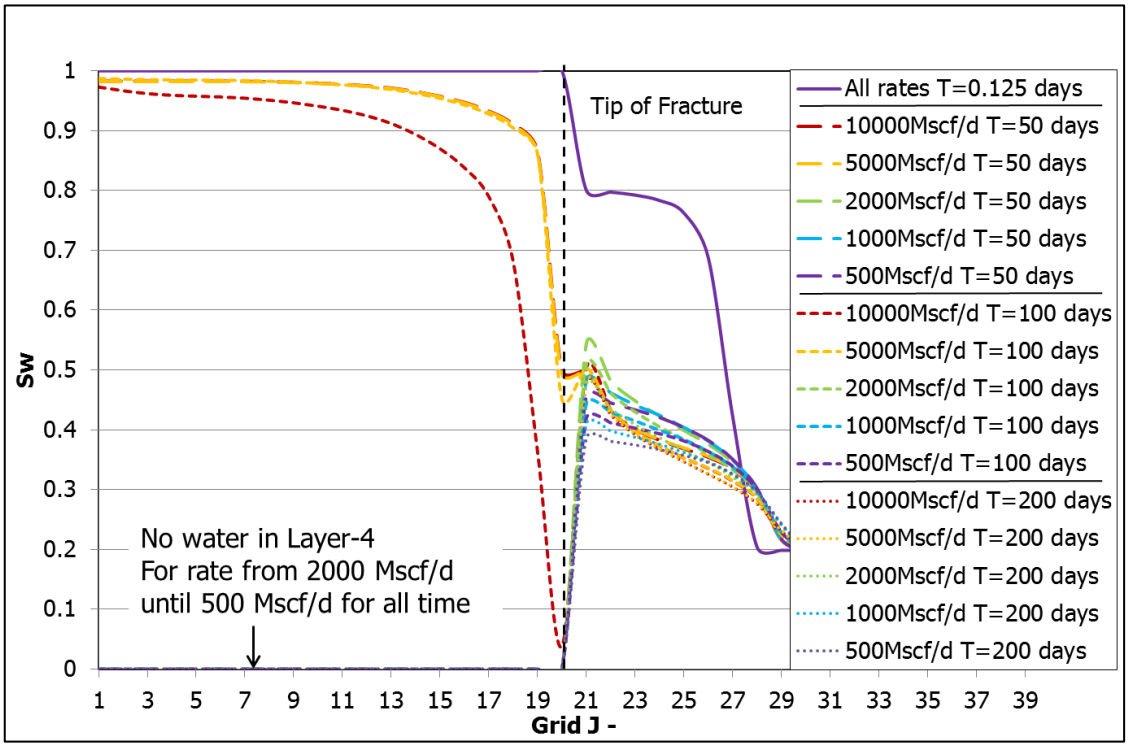

Figure 3. 38 – Sensitivity of Rate with Water Constrain in Layer-4: Water Saturation Profile (JK-cross section, I=15)

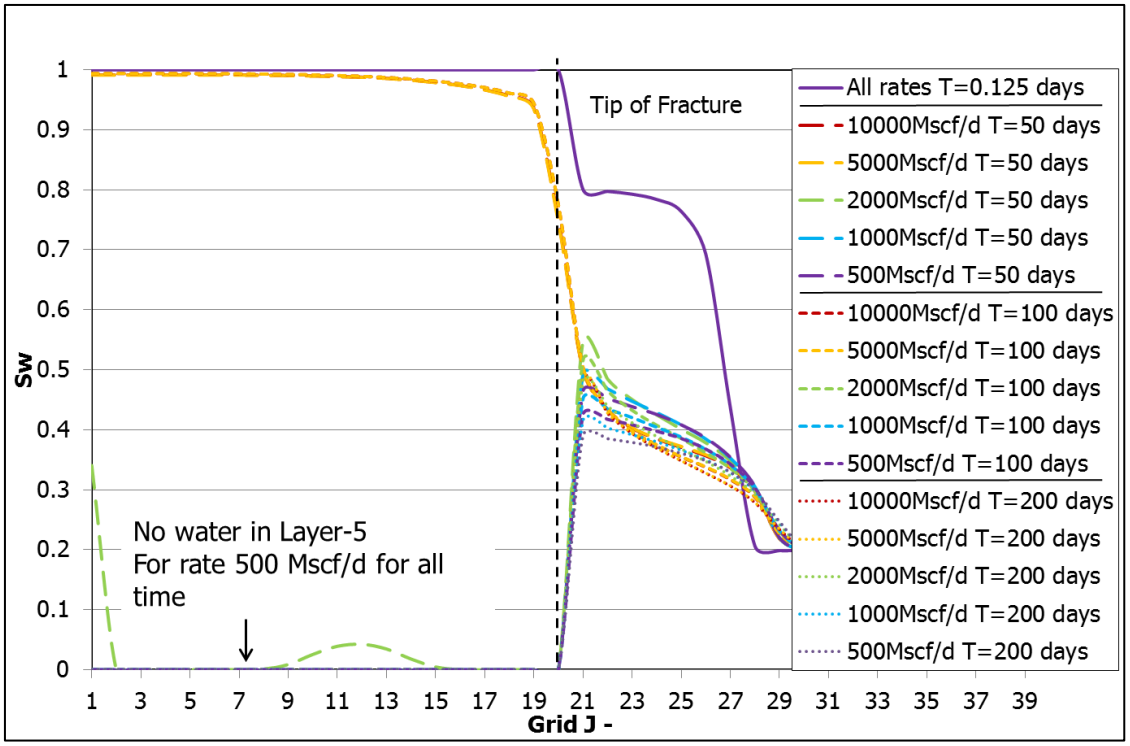

Figure 3. 39 – Sensitivity of Rate with Water Constrain in Layer-5: Water Saturation Profile (JK-cross section, I=15)

3.5.1.2 Production Profile

Figure 3.40 shows the gas production profile for different gas rates. For the first 10 days of production, gas production rate and cumulative gas production profile are the same for all cases because of the same water production constrain. After 10 days, constrain for the production was changed to a constant bottomhole pressure of 1,500 psi. Plateau rate is observed for the gas rate less than 5,000 Mscf/d. It can also be seen that the gas production profile for 5,000 Mscf/d and 10,000 Mscf/d is relatively similar. A gas rate limit where the deliverability of the well is similar may exist.

Water production profile for different gas rate can be seen in **Figure 3.41**. If we see the profile for the gas rate 500 Mscf/d, 1,000 Mscf/d and 2,000 Mscf/d, water is only produced for the first 10 days. There is no water production afterwards. If we compare the production profile with the water saturation profile analysis, it also can be seen no water presence is observed for the rates below 2,000 Mscf/d in all fracture layers. So that after 10 days of production, cumulative water production is the same and constant until the end of simulation.

Water rate profiles for the gas rate 5,000 Mscf/d and 10,000 Mscf/d follow its gas production profiles. Although the end of water production for the gas rate 10,000 Mscf/d case is faster than the gas rate 5,000 Mscf/d case, its cumulative water production is still higher than other case. But the difference is insignificant.

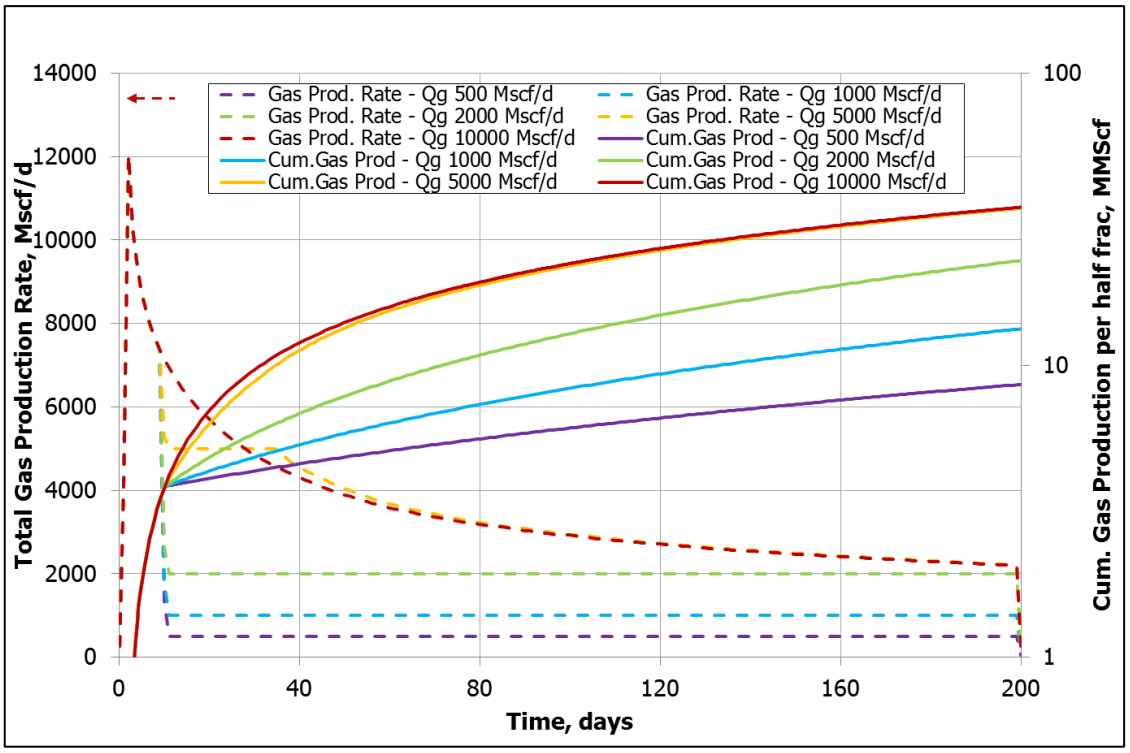

Figure 3. 40 – Sensitivity of Rate with Water Constrain: Gas Production Profile

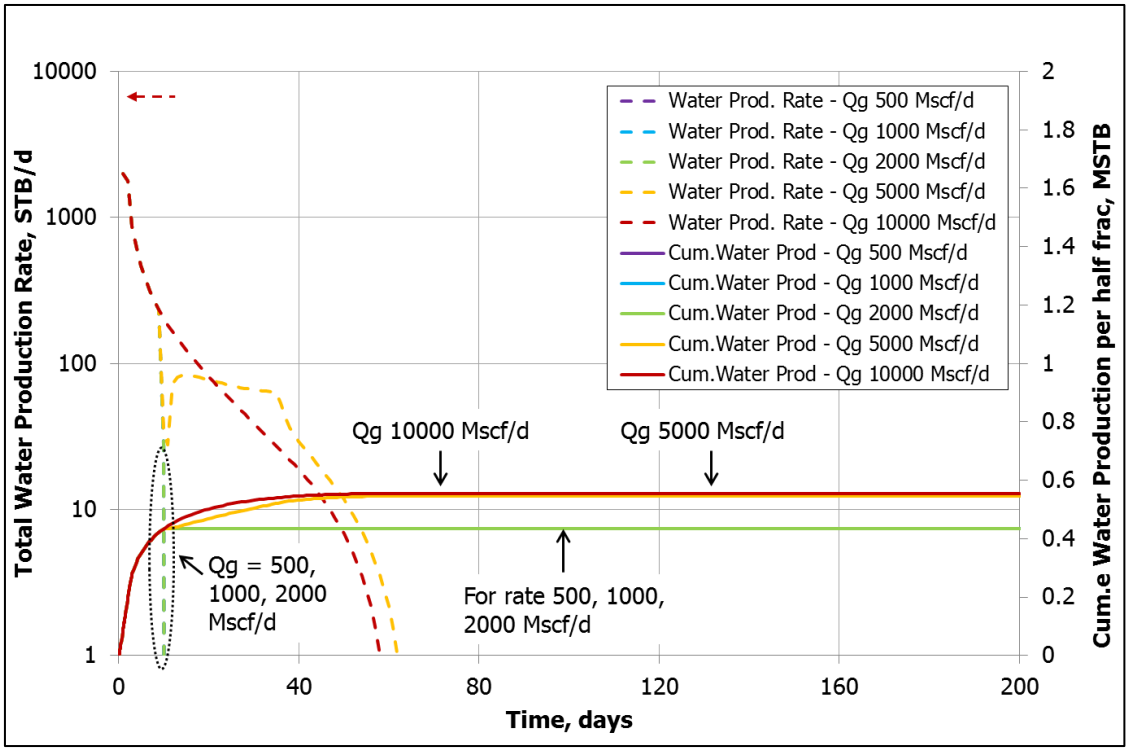

Figure 3. 41 – Sensitivity of Rate with Water Constrain: Water Production Profile

3.5.2 Rate Sensitivity without Water Constrain

In this section, water constrain was not applied for the rate sensitivity. There was no water production limit for the simulation. The well was only controlled by a constant bottomhole pressure of 1,500 psi.

3.5.2.1 Water Saturation Profile

Water saturation profile for this sensitivity cases has practically the same profile as the profiles from the sensitivity rate with water constrain. There are some new observations from this sensitivity. As shown in **Figure 3.42** until **Figure 3.46**, comparing water saturation profile for the gas rate 5,000 Mscf/d and 10,000 Mscf/d in this sensitivity with previous water saturation analysis for the cases with water constrain, it shows almost the same behavior. Water presence is observed from layer-2 to layer-5 of the fracture for these two rate cases.

When water constrains is not applied, water presence in the fracture is also observed for the case with gas rate 2,000 Mscf/d. It observes from layer-2 to layer-5 of the fracture. If we see water saturation in layer-3, layer-4, and layer-5 of the fracture for the case with gas rate

2,000 Mscf/d, its water saturation is higher than water saturation for the higher gas rate cases. It suspects the water from the matrix reaches the fracture but the gas rate may be insufficient to lift the water as fast as higher gas rates.

For the case with gas rate 1,000 Mscf/d water saturation is only observed at layer-5 of the fracture. Water saturation is quite high in the grid J=1 until J=14. The water flowback from the matrix fills the fracture, but the gas rate may too low to push the water to be produced. There is no water presence for this rate at the upper fracture layers.

Water saturation equals zero is observed for the gas rate 500 Mscf/d in the fracture after water injection. Water in the fracture is all produced when the production is started and the water is also trapped in the matrix near the fracture face.

At t=200 days in all fracture layers for all cases, fracture is free from the water since water saturation is observed zero.

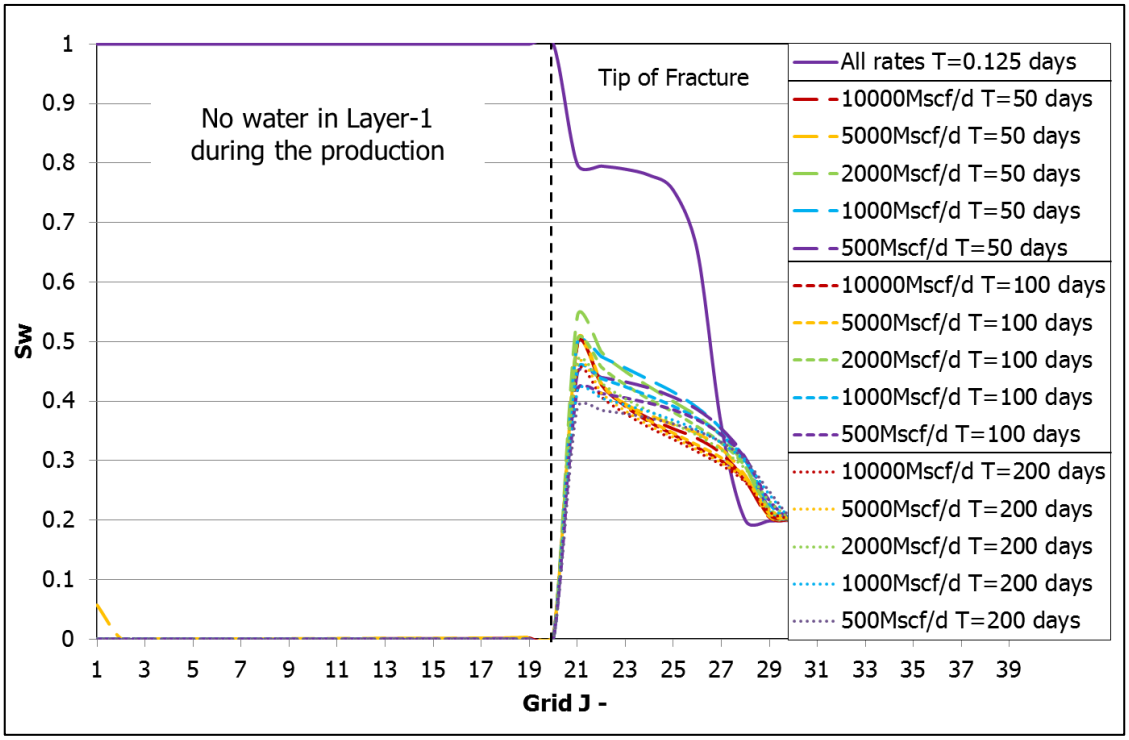

Figure 3. 42 – Sensitivity of Rate without Water Constrain: Water Saturation Profile in Layer-1 (JK-cross section, I=15)

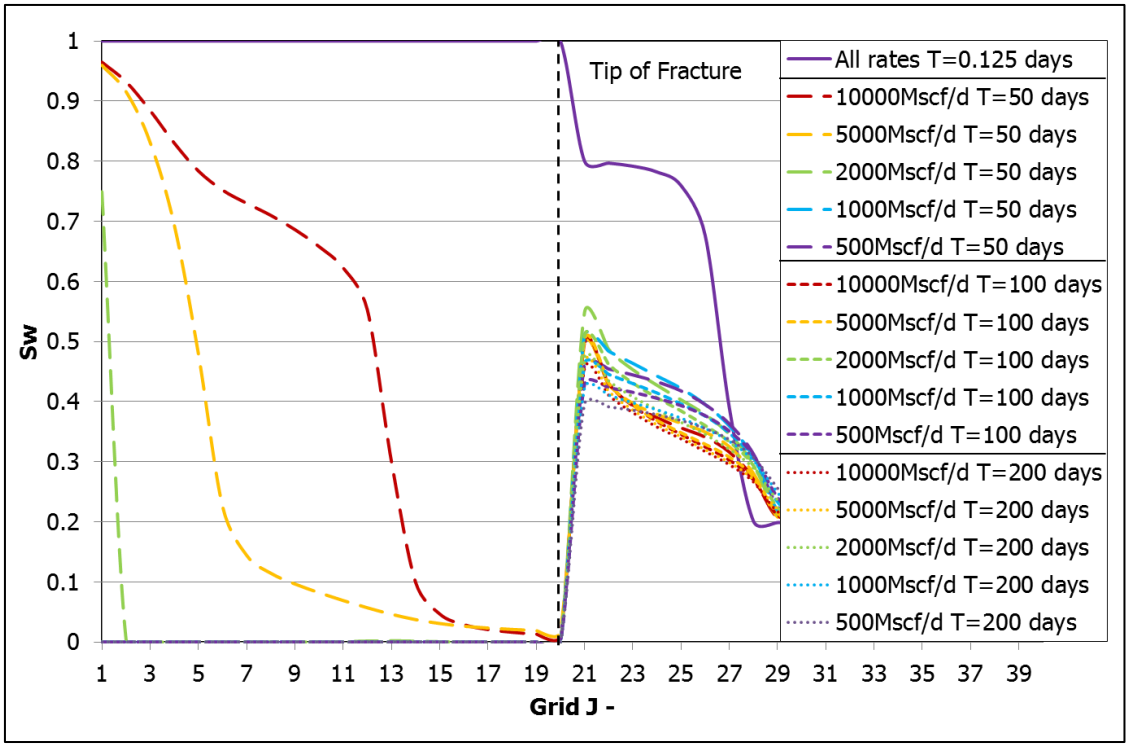

Figure 3. 43 – Sensitivity of Rate without Water Constrain: Water Saturation Profile in Layer-2 (JK-cross section, I=15)

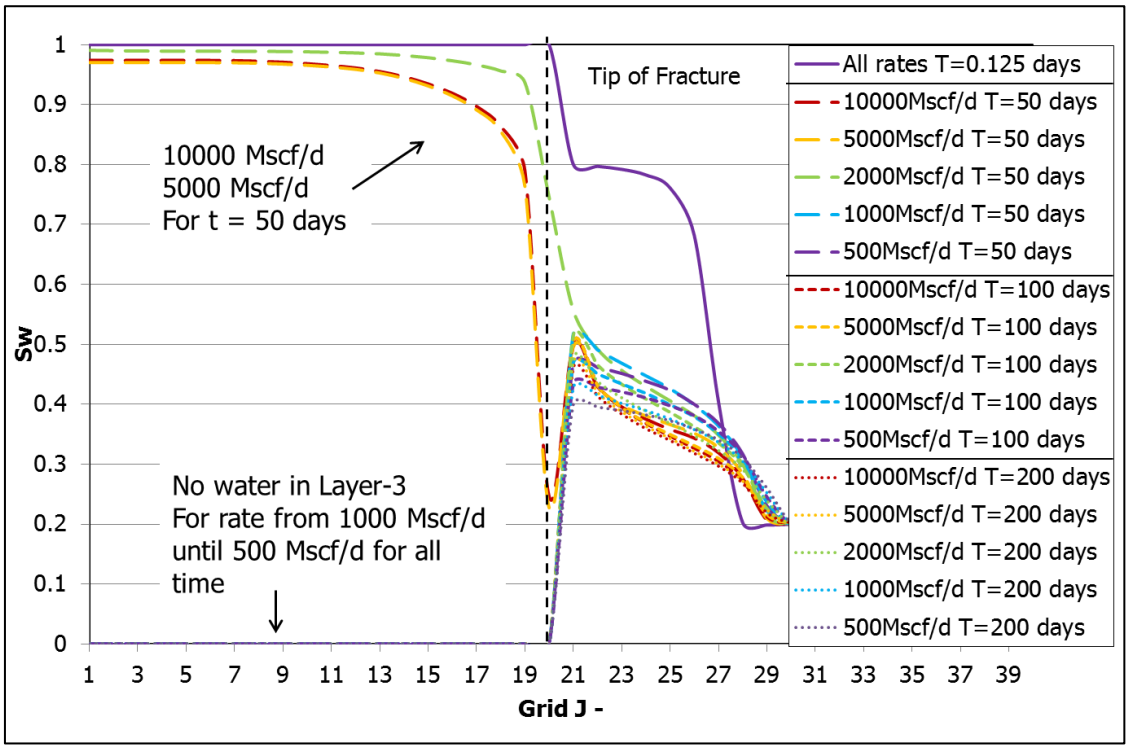

Figure 3. 44 – Sensitivity of Rate without Water Constrain: Water Saturation Profile in Layer-3 (JK-cross section, I=15)

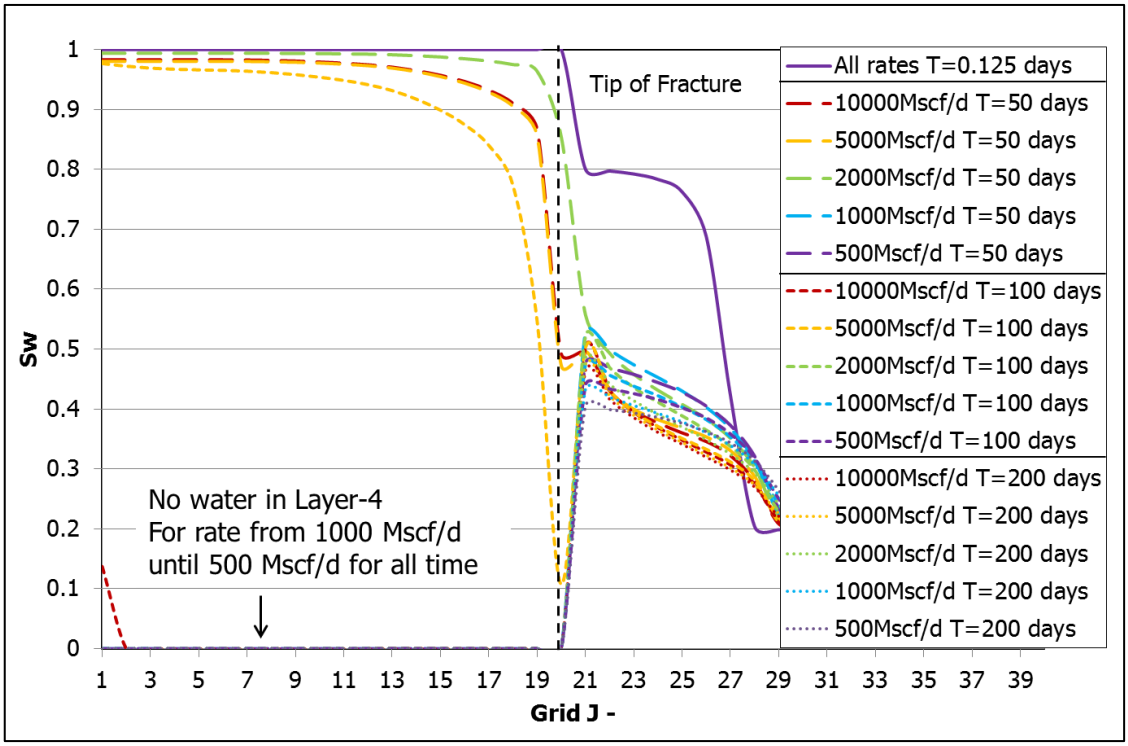

Figure 3. 45 – Sensitivity of Rate without Water Constrain: Water Saturation Profile in Layer-4 (JK-cross section, I=15)

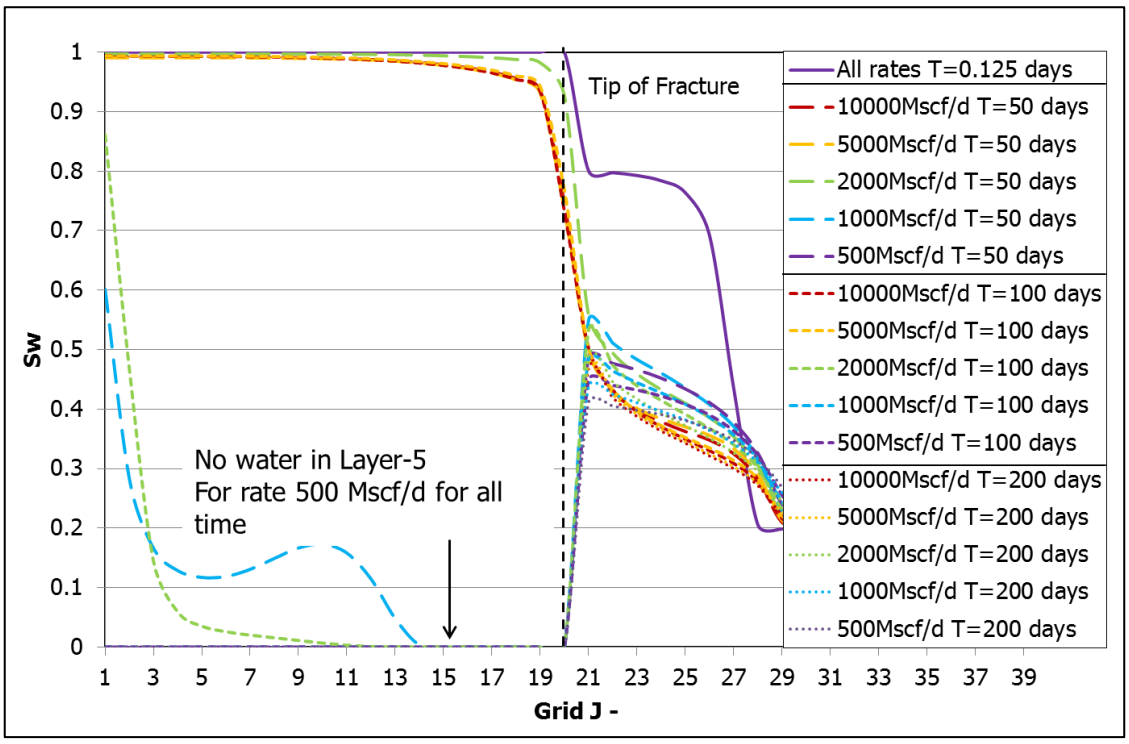

Figure 3. 46 – Sensitivity of Rate without Water Constrain: Water Saturation Profile in Layer-5 (JK-cross section, I=15)

3.5.2.2 Production Profile

Figure 3.47 shows the gas production profile for these sensitivities. Plateau rate is observed for the case with gas rate is below 5,000 Mscf/d. There is a similar behavior for the case with gas rate 5,000 Mscf/d and 10,000 Mscf/d. The cumulative gas production for these two cases is almost similar. An upper gas rate limit where the deliverability of the well is similar may exist.

Water production profile for these sensitivities can be seen in **Figure 3.48**. For the gas rate 500 Mscf/d and 1,000 Mscf/d, water production is observed less than 10 production days. As can be seen in the water saturation analysis for this case, water is not observed for these two rates in almost all layer at t>50 days. Although water presence is observed for gas rate 1,000 Mscf/d in layer-5 of the fracture at t=50 days in the water saturation analysis, it could be immobile water. From this analysis, it can be seen that lower gas rate results in lower water production.

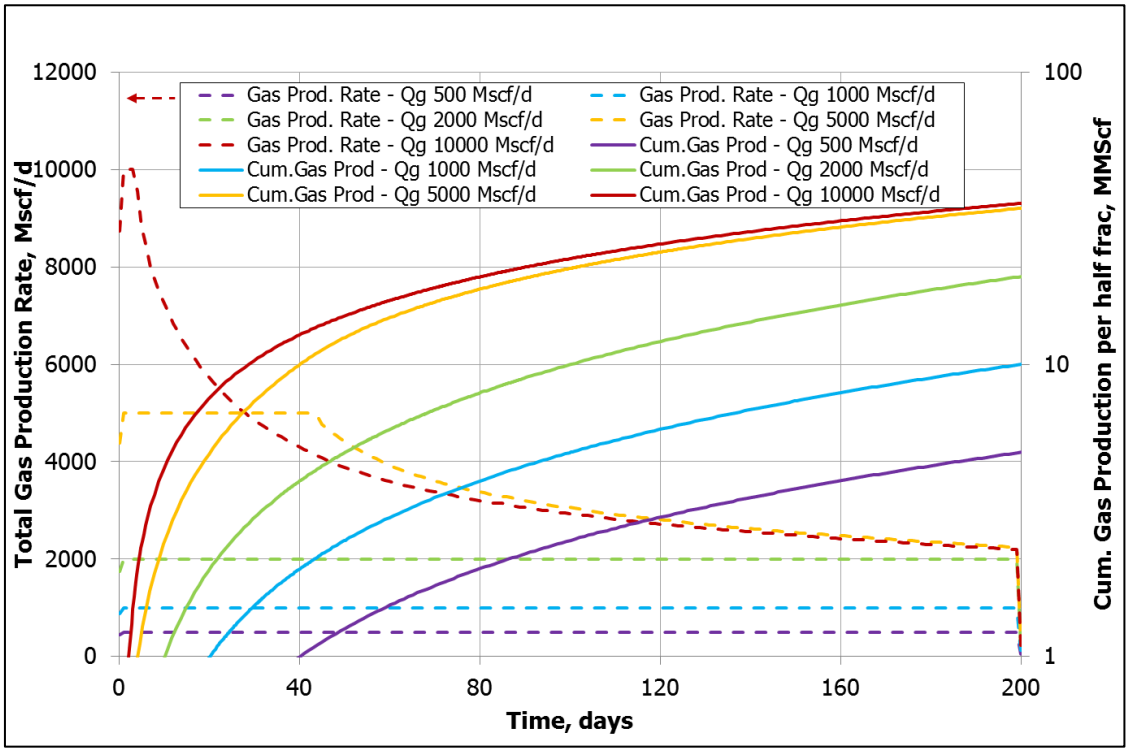

Figure 3. 47 – Sensitivity of Rate without Water Constrain: Gas Production Profile

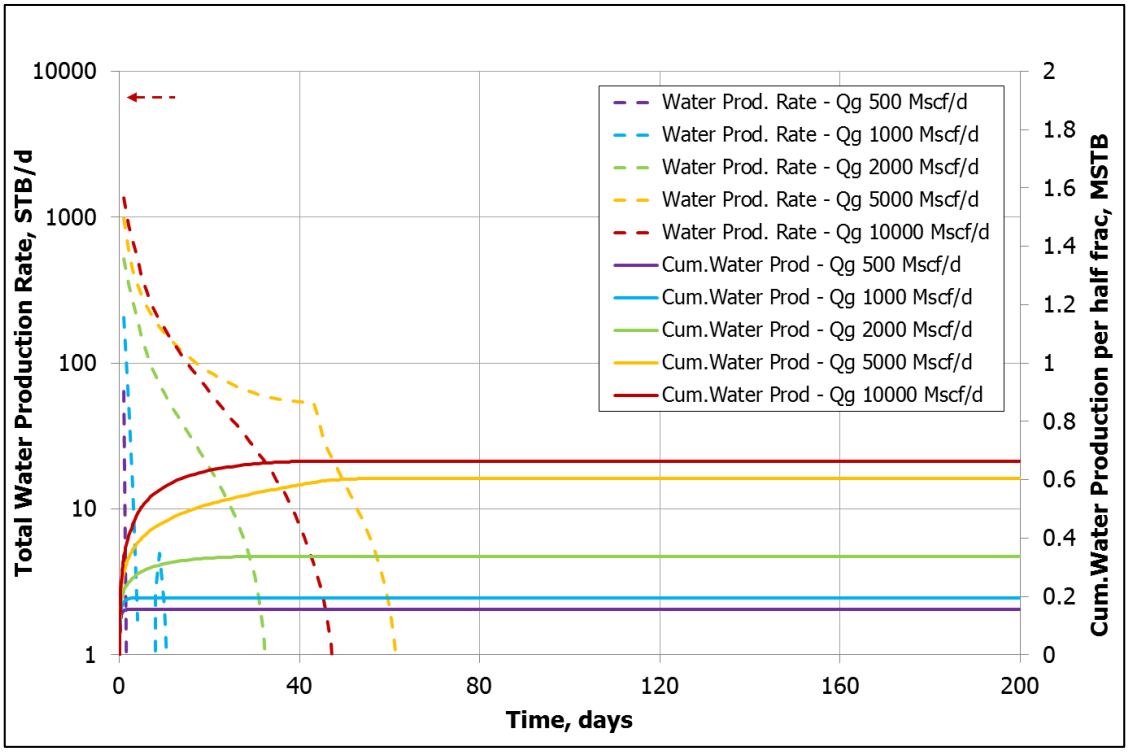

Figure 3. 48 – Sensitivity of Rate without Water Constrain: Water Production Profile

3.6 Shut-In Sensitivity

In this part, shut-in period was applied for the base case after water injection. Water constrain for the first 10 days was still applied for this sensitivity. Two different shut-in periods were run to see its effect on water saturation in the fracture. The effect on production profiles were also the other objective. The shut-in cases are:

1. The well is shut-in for 15 days after water injection and is opened afterwards.
2. The well is shut-in for 30 days after water injection and is opened afterwards.

3.6.1 Water Saturation Profile

Figure 3.49 until **Figure 3.53** shows water saturation profile for each case in different layer and different time. For all cases, after water injection (t=0.125 days) fracture is filled with water (S_w=1).

Water saturation is zero at layer-1 of the fracture for all cases and after water injection. For the base case, water saturation in layer-2 of the fracture decreases along with the production.

For the cases with shut-in, water saturation in layer-2 of the fracture is also observed decreasing along with production. The water production is delayed because of shut-in period. For the case with shut-in 30 days, water saturation at t=50 days is smaller than t=100 days. Water from the matrix still feeds the fracture along with the production.

For layer-3 of the fracture, water saturation for base case and shut-in cases are observed high for t=50 days and t=100 days. Layer-4 of the fracture shows the same trend water saturation as can be seen in layer-3 of the fracture. Water saturation is still high for all cases at t=50 days and t=100 days. But for the base case at t=100 days, water saturation decreases faster compared to other cases. High water saturation for shut-in cases indicate delayed of the water production.

For layer-5 of the fracture, all cases have high water saturation during production. At t=200 days for shut-in cases, water presence is still observed in the grids near the well. If we compare it to the base case at t=200 days, delayed water production due to shut-in causes water saturation still can be seen. The water at this layer for t=200 days is expected to be immobile water. Because in the upper layer of the fracture, water saturation at t=200 days is zero.

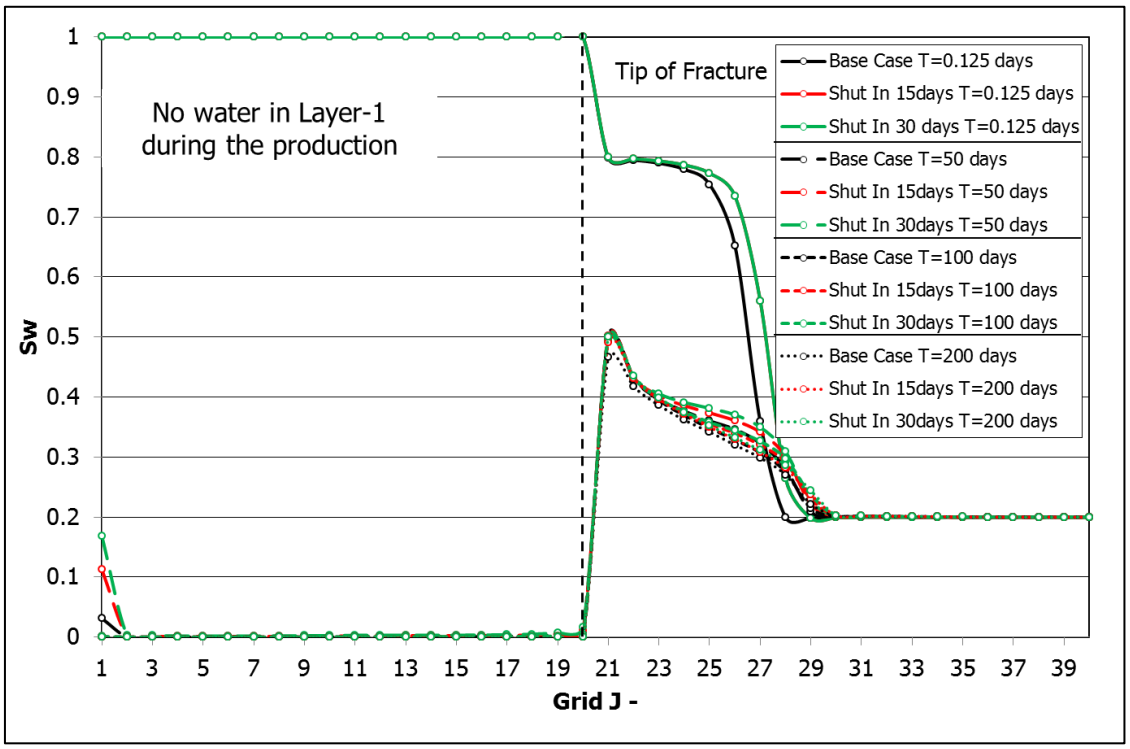

Figure 3. 49 – Sensitivity of Shut-In: Water Saturation Profile in Layer-1 (JK-cross section, I=15)

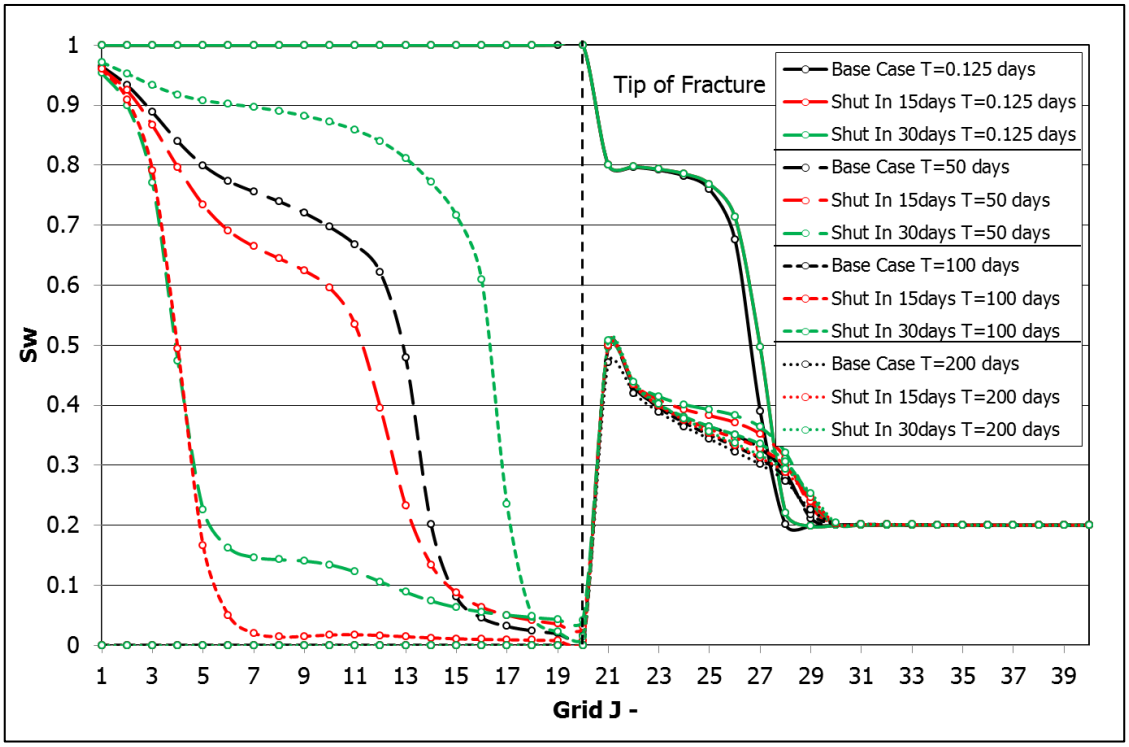

Figure 3. 50 – Sensitivity of Shut-In: Water Saturation Profile in Layer-2 (JK-cross section, I=15)

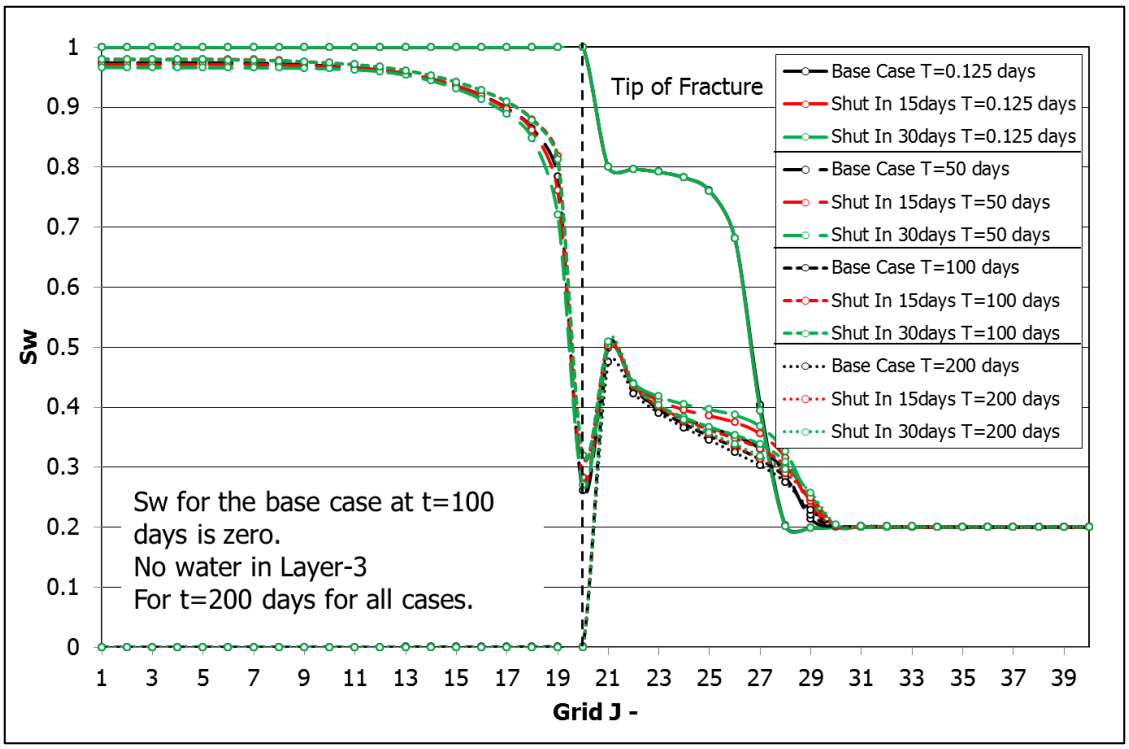

Figure 3. 51 – Sensitivity of Shut-In: Water Saturation Profile in Layer-3 (JK-cross section, I=15)

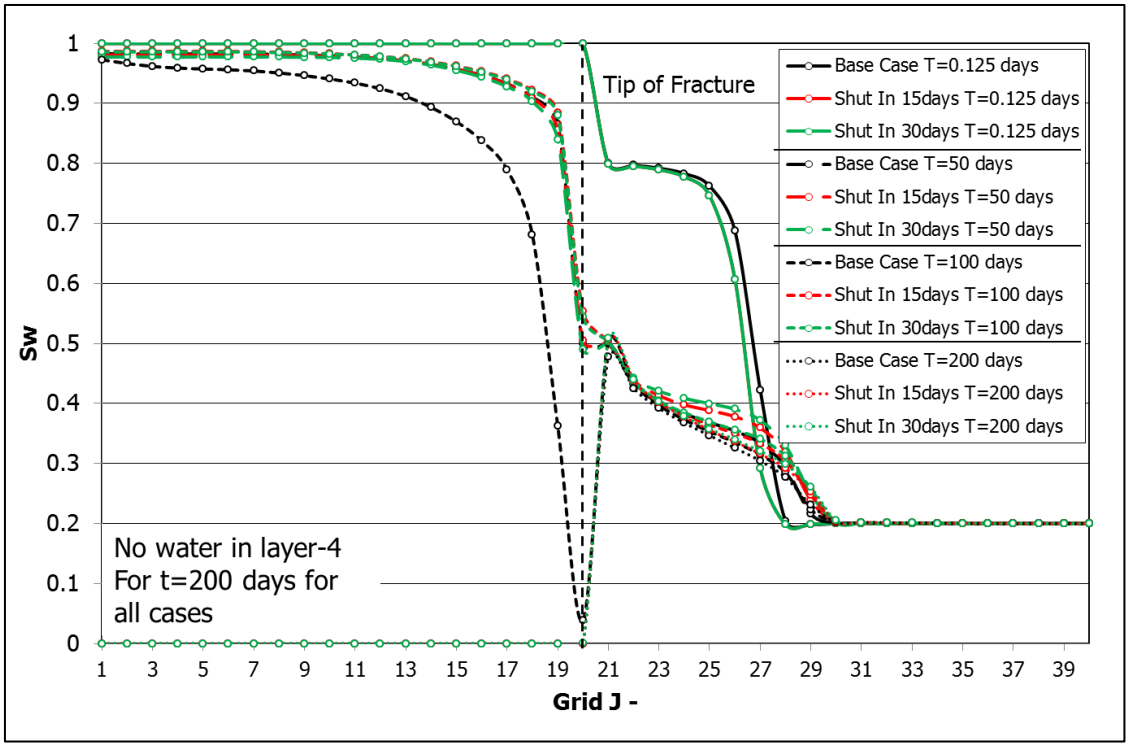

Figure 3. 52 – Sensitivity of Shut-In: Water Saturation Profile in Layer-4 (JK-cross section, I=15)

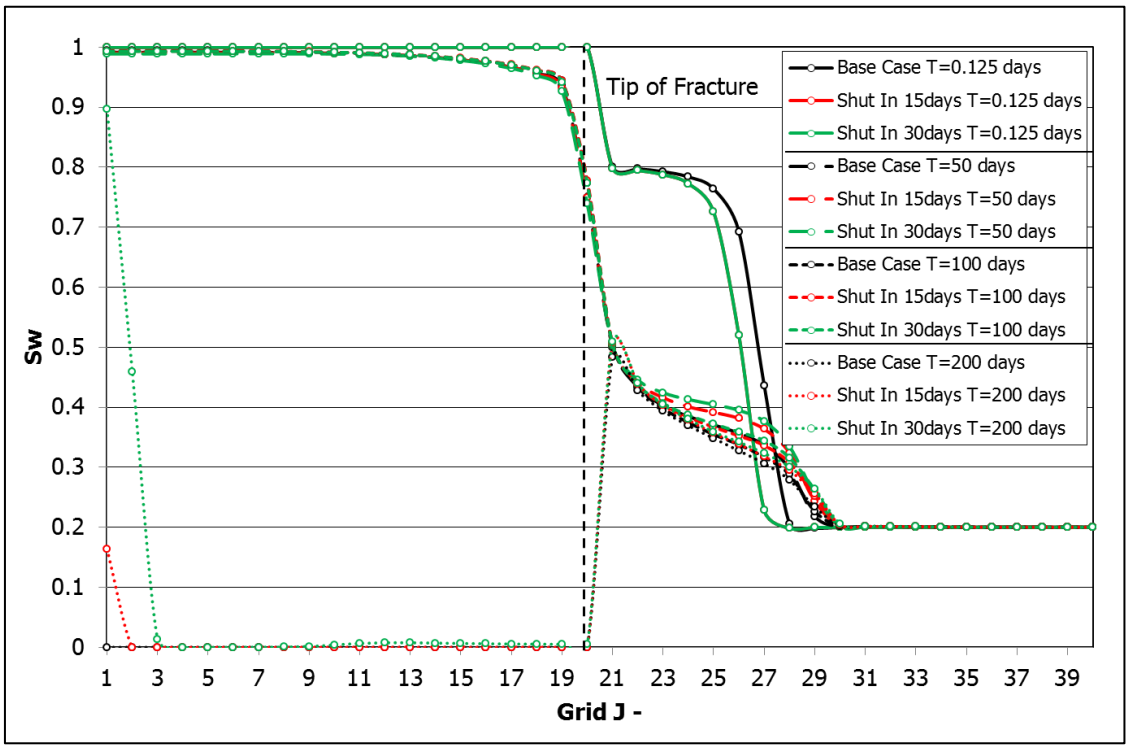

Figure 3. 53 – Sensitivity of Shut-In: Water Saturation Profile in Layer-5 (JK-cross section, I=15

3.6.2 Production Profile

Gas production profile can be seen in **Figure 3.54**. Gas production is delayed for two shut-in cases. But when the well is opened for shut-in cases, higher initial gas rate is observed. For shut-in cases, water imbibes deeper to the formation. It affects different water saturation distribution in the matrix during the production. Therefore, the gas production rate may be different due to different relative permeability. For all cases, gas rate decline shows the same trend after 120 production days. For the base case, gas recovery factor is 2.325%. While for the case with 15 days shut-in is 2.149% and for the case with 30 days shut-in is 2.016%.

The plot in **Figure 3.55** shows the water production profile. Shut-in cases shows lower initial water rate. So that cumulative water production is significantly different. For the shut-in case, water imbibes deeper into the formation. Water recovery until 200 production days for the base case is 0.5541 MSTB or 27.7% of injected water is recovered. While for the case with 15 days shut-in is 15.3% and for the case with 30 days shut-in is 10.05%.

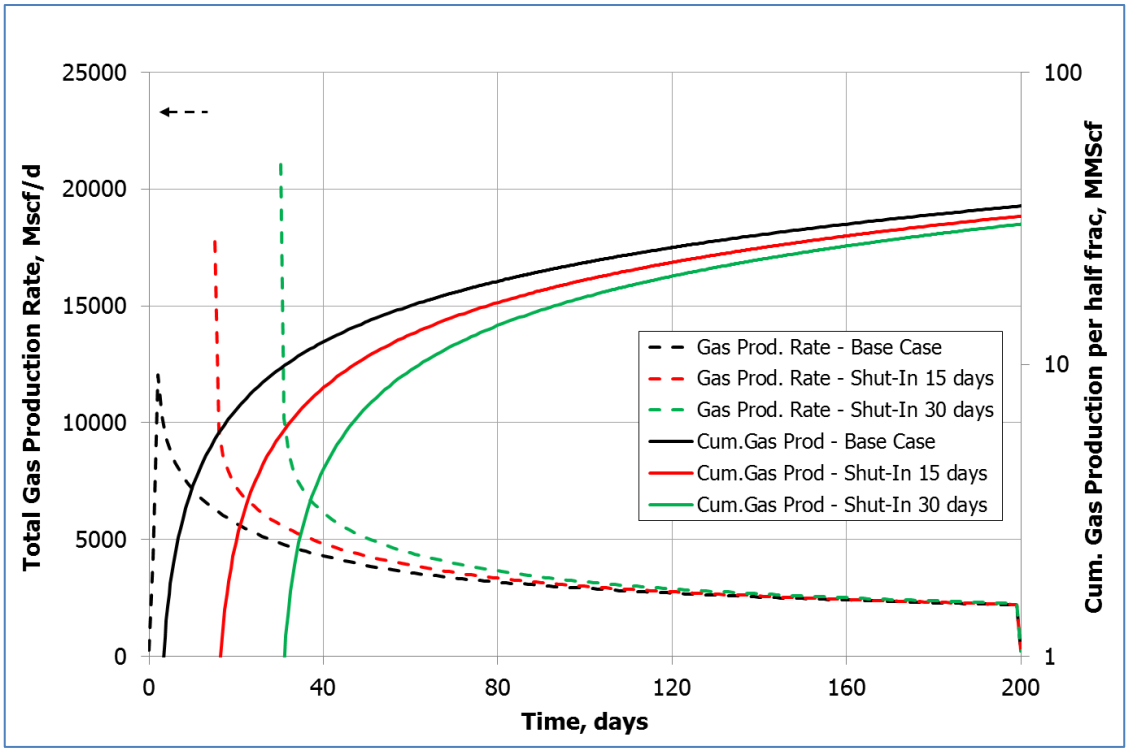

Figure 3. 54 – Sensitivity of Shut-In: Gas Production Profile

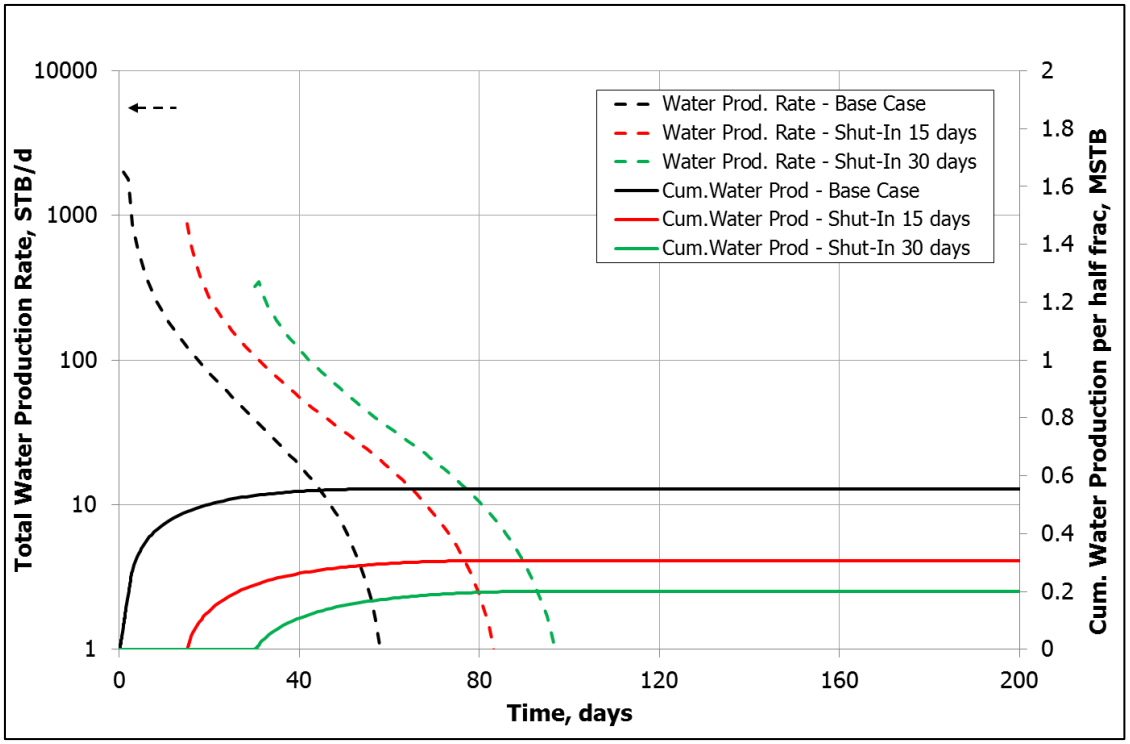

Figure 3. 55 – Sensitivity of Shut-In: Water Production Profile

Chapter 4

Summary and Recommendation

A hydraulically-fractured shale gas well model, which include layering and stress dependent permeability, has been built using Sensor through Pipe-It Shale Well Optimizer. The model consists of a horizontal well with 10 fractures, but only a half fracture zone was modeled because of symmetry. As each fracture behaves independently, only one side of the fracture was modeled.

Water behavior in the fracture was studied through water saturation profile in the fracture grids. Sensitivities were applied to the model and its consequent results analyzed. Both fracture water saturation and production profiles were observed to compare the effects of different properties and constrains.

From this study, the following conclusions are presented. According to the number of layer sensitivity, a five layers model is enough to represent the model for this study. The base case model showed that fracture is filled with water after water injection and the water saturation in the fracture decreases with production. The fracture is also free from the water after some of production time, which in this study is observed at the end of simulation.

The uppermost fracture layer has the lowest water saturation, while the lowermost fracture layer has the highest water saturation. This is a possibility observed due to segregation in the fracture. Production commencing after water injection would result in water within the fracture is produced with the gas. If shut-in is performed or well is produced with a low rate, the water imbibes into the formation.

Perforation location has impact on water saturation profile in the fracture, but has insignificant effect on the overall production profile. When the lowermost layer is perforated, it results in

low water saturation in all fracture layers. However, water production is higher in this case as compared to an opposing result of lower water production in uppermost layer perforation case. In contrast, the location of perforation has an insignificant effect on gas production.

Reservoir with heterogeneity between layers, especially with different permeability values, has a noteworthy influence to the water saturation profile in the fracture. Reservoir with high permeability in the uppermost layer gives higher water saturation in the fracture. It also allows for a slightly higher water production and slightly higher gas production compared to the reservoir with high permeability in the lowermost layer, despite that the differences in the production are not that significant. An important note on matrix permeability sensitivity, the total *kh* for the model is maintained at a constant.

Different gas rates correspond to different water saturation in the fracture. This analysis conducted suggests that there may be a critical gas rate to feed the water from the matrix to the fracture. If there is water present in the fracture for the low gas rate, the water tends to be immobile or re-imbibes into the formation due to low gas rate. Therefore, higher gas rate results in higher water production.

Shut-in period after water injection has an insignificant effect on water saturation profile in the fracture. It is observed, however that the water feed from the matrix to the fracture is slightly delayed. Water imbibes deeper into the formation when shut-in period applied. Initial gas rate for the shut-in cases is observed higher than the base case, the case without shut-in period. The production with shut-in period after water injection has slightly lower gas production total, but the difference is insignificant. Shut-in period after water injection definitely has a significant effect on the water production profile, as compared to immediate production upon water injection. The shut-in cases results in a lower water production rate initial, so that the total water production for the shut-in cases is lower than the base case.

Water presence in the fracture is only observed during the first period of the production. It decreases along with the production. The difference is contributed by the time needed to clean-up the water from the fracture. Lower water recovery also indicates deeper water imbibition into the formation.

It would be interesting to conduct further study on the water behavior around the fracture face. The current study suggests that water saturation in the matrix near the fracture face is high during the production. The matrix near the fracture face does not start cleaning-up until the capillary pressure barrier is overcome. It is with hopes that this study could lead on to a deeper analysis on how the water in the matrix near the fracture face affects the production and its manner of feeding water to the fracture.

Nomenclature

h = thickness, ft
k = permeability, md
$\bar{k}$ = average permeability, md
k_o = original matrix permeability, md
m = permeability enhancement factor, psi^{-1}
p_{net} = net pressure (difference between grid cell pressure & initial reservoir pressure), psi
Q_g = gas rate, Mscf/d
S_w = water saturation
t = time, days
$\sum$ = sum of squares

Reference

[1] Agrawal, S. and Sharma, M. M. *Impact of Liquid Loading in Hydraulic Fractures on Well Productivity*. Paper SPE 163837 presented at the SPE Hydraulic Fracturing Technology Conference, The Woodlands, Texas, USA, 4 – 6 January 2013

[2] Boyer, C. et al. *Shale Gas: A Global Resource*. Oilfield Review Autumn 2011: 23, no.3, pp. 28-39, Schlumberger, 2011.

[3] Coats Engineering, Inc. *Sensor Compositional and Black Oil Reservoir Simulation Software,* http://coatsengineering.com/sensor_reservoir_simulator.htm, 2013

[4] Coats Engineering, Inc. *Sensor Manual*, 2011.

[5] Jurus, W., Whitson, C.H, and Golan, M. *Modeling Water Flow in Hydraulically-Fractured Shale Wells*. Paper SPE 166439 presented at the SPE Annual Technical Conference and Exhibition, New Orleans, Louisiana, USA, 30 September – 2 October 2013

[6] Petrostreamz A/S. http://www.petrostreamz.com/pipe-it . 2013

[7] Petrostreamz A/S. *Case Studies.* http://www.petrostreamz.com/case-studies . 2013

[8] Whitson, C. H. *e-notes*. http://www.ipt.ntnu.no/~curtis/courses/PVT-Flow/e-notes . 2013

[9] Whitson, C. H., and Sunjerga, S. *PVT in Liquid-Rich Shale Reservoirs*. Paper SPE 155499 presented at the SPE Annual Conference and Exhibition, San Antonio, Texas, USA, 8 – 10 October 2012

Appendix

Base Case Sensor Main Input Date

```
TITLE
INCLUDE
..\Title.inc
ENDTITLE

INCLUDE
..\Grid-RelPerm.inc

C ---------------------------------------------------------------------
C Black oil table
C ---------------------------------------------------------------------
PVTBO

C               deno    deng    coil    cvoil
DENSITY         0.8     0.7     0       0

PRESSURES     1 44
15.0    25.0    50.0    75.0    100.0   125.0   150.0   175.0   200.0
225.0   250.0   300.0   350.0   400.0   490.0   500.0   550.0   600.0
650.0   700.0   750.0   800.0   850.0   900.0   950.0   1000.   1500.
2000.   2500.   3000.   3500.   4000.   4500.   5000.   5500.   6000.
6500.   7000.   7500.   8000.   8500.   9000.   9500.   10000.

PSAT    SRS
15.0    0.0

C psia          RB/scf          cp
P               BG              VISG
15              0.2210427       0.01305
25              0.1325079       0.01305
50              0.0661055       0.01307
75              0.0439723       0.01309
100             0.0329061       0.01311
125             0.0262667       0.01313
150             0.0218408       0.01315
175             0.0186796       0.01317
200             0.0163090       0.01320
225             0.0144653       0.01322
250             0.0129906       0.01325
300             0.0107790       0.01331
350             0.0091998       0.01337
400             0.0080159       0.01344
490             0.0064948       0.01356
500             0.0063597       0.01358
550             0.0057580       0.01365
600             0.0052570       0.01373
650             0.0048334       0.01381
700             0.0044707       0.01390
750             0.0041567       0.01399
```

```
800             0.0038822       0.01408
850             0.0036403       0.01417
900             0.0034257       0.01427
950             0.0032339       0.01437
1000            0.0030615       0.01447
1500            0.0019818       0.01566
2000            0.0014604       0.01712
2500            0.0011639       0.01880
3000            0.0009795       0.02061
3500            0.0008574       0.02247
4000            0.0007723       0.02432
4500            0.0007104       0.02613
5000            0.0006635       0.02787
5500            0.0006269       0.02954
6000            0.0005974       0.03115
6500            0.0005732       0.03269
7000            0.0005528       0.03416
7500            0.0005355       0.03559
8000            0.0005205       0.03696
8500            0.0005074       0.03828
9000            0.0004958       0.03956
9500            0.0004854       0.04081
10000           0.0004761       0.04201

C -----------------------------------------------------------------
C Stress dependent trans.
C -----------------------------------------------------------------
INCLUDE
 ..\stress.inc

TMODTYPE CON
 1
 MOD
 15 15 1 20 1 1 = 2

DATE 01 01 2013

C -----------------------------------------------------------------
C Initialize
C -----------------------------------------------------------------
INITIAL

C DEPTH GOR
C 13538 9880

INCLUDE
..\well.inc

C -----------------------------------------------------------------
C Define rate schedules.
C -----------------------------------------------------------------

INCLUDE
 schedule.inc

END
```

Sensor Include Data File (Grid-RelPerm.inc)

```
GRID 29 40 5
PCMULT2 1. 0.
RUN
CPU
IMPLICIT

MAPSPRINT 1 P SO SW KX
MAPSFILE P SW SO SG

C       Bwi     cw      denw    visw    cr      pref
MISC    1       3.0E-6  62.4    0.5     4.0E-6  6000

C -----------------------------------------------------------------
C Including grid definition created by SensorGrid
C -----------------------------------------------------------------
INCLUDE
 ..\initial.inc

C -----------------------------------------------------------------
C Relperm
C -----------------------------------------------------------------

KRANALYTICAL 1    ! For matrix
 0.2 0.2 0.0 0.2                ! Swc Sorw Sorg Sgc
 1 1 1                          ! krw(Sorw) krg(Swc) kro(Swc)
 2.5 2.5 2.5 2.5                ! nw now ng nog
 0 3480 5  PCWO                 ! a1 a2 a3
 0 3480 5 0 0  PCWOI            ! b1 b2 b3 b4 b5
 -10 10 1. PCGO                 ! c1 c2 c3

 KRANALYTICAL 2   ! For fractures
 0 0 0 0                        ! Swc Sorw Sorg Sgc
 1 1 1                          ! krw(Sorw) krg(Swc) kro(Swc)
 1 1 1 1                        ! nw now ng nog
C 0 3480 20  PCWO               ! a1 a2 a3
C 0 3480 20 3480 2  PCWOI       ! b1 b2 b3 b4 b5
 -10 10 1. PCGO                 ! c1 c2 c3
```

Sensor Include Data File (Initial.inc)

```
C ---------------------------------
C I_CELLS          29
C J_CELLS          40
C K_CELLS           5
C DEPTH            10000
C SYM_ELEMENTS      2
C FRAC_AREA        60000
C ---------------------------------

C ------------------------------------------------------------------
C Cell width along wellbore
C ------------------------------------------------------------------
DELX XVAR
115.705          62.1544          33.3881          17.9354          9.63454          5.17548
2.78016          1.49345          0.80225          0.430952         0.231499         0.124356
0.0668018        0.0358846        0.0833           0.0358846        0.0668018        0.124356
0.231499         0.430952         0.80225          1.49345          2.78016          5.17548
9.63454          17.9354          33.3881          62.1544          115.705

C ------------------------------------------------------------------------------------------
C Cell width away from wellbore
C ------------------------------------------------------------------------------------------
DELY YVAR
100.827          66.9495          44.4547          29.518           19.6001          13.0145
8.64168          5.7381           3.81012          2.52993          1.67988          1.11545
0.74066          0.491801         0.326557         0.216835         0.143979         0.0956026
0.0634804        0.0421512        0.0439198        0.0670764        0.102442         0.156455
0.238945         0.364929         0.557337         0.851192         1.29998          1.9854
3.03219          4.63091          7.07255          10.8015          16.4966          25.1944
38.4782          58.7657          89.7499          137.07

C ------------------------------------------------------------------
C Porosity
C ------------------------------------------------------------------
POROS ZVAR
0.1      0.1      0.1      0.1      0.1

MOD
15 15 1 20 1 5 = 0.030012


C ------------------------------------------------------------------
C Rocktype (for relperm curves)
C ------------------------------------------------------------------
ROCKTYPE CON
 1

MOD
15 15 1 20 1 5 = 2

C ------------------------------------------------------------------
C Permeability
C ------------------------------------------------------------------
```

KX ZVAR
0.0002 0.0002 0.0002   0.0002 0.0002

MOD
15 15 1 20 1 5 = 12004.8

KY EQUALS KX
KZ EQUALS KX

C ---
C Depth
C ---
DEPTH CON
10000

C ---
C Thickness
C ---
THICKNESS ZVAR
40 40 40 40 40

Sensor Include Data File (Stress.inc)

C Model: k/ko=10^(-m*(stress/ref pres))
C m = 1.15x10^-3
TMODTABLE 1
5000 0

C stress	TXMOD	TYMOD	TZMOD
-3500	10592.5372517729	10592.5372517729	10592.5372517729
-3383.33333333333	7777.38025764418	7777.38025764418	7777.38025764418
-3266.66666666667	5710.40178894528	5710.40178894528	5710.40178894528
-3150	4192.75996684607	4192.75996684607	4192.75996684607
-3033.33333333333	3078.4587125933	3078.4587125933	3078.4587125933
-2916.66666666667	2260.30302714192	2260.30302714192	2260.30302714192
-2800	1659.58690743756	1659.58690743756	1659.58690743756
-2683.33333333333	1218.5218841302	1218.5218841302	1218.5218841302
-2566.66666666667	894.677811357748	894.677811357748	894.677811357748
-2450	656.901116476265	656.901116476265	656.901116476265
-2333.33333333333	482.317848223929	482.317848223929	482.317848223929
-2216.66666666667	354.133218654328	354.133218654328	354.133218654328
-2100	260.015956316526	260.015956316526	260.015956316526
-1983.33333333333	190.912046591118	190.912046591118	190.912046591118
-1866.66666666666	140.173741834676	140.173741834676	140.173741834676
-1750	102.920052719442	102.920052719442	102.920052719442
-1633.33333333333	75.5672004837097	75.5672004837097	75.5672004837097
-1516.66666666666	55.4838599287508	55.4838599287508	55.4838599287508
-1400	40.7380277804109	40.7380277804109	40.7380277804109
-1283.33333333333	29.9111653293169	29.9111653293169	29.9111653293169
-1166.66666666666	21.9617360020541	21.9617360020541	21.9617360020541
-1050	16.1250102733772	16.1250102733772	16.1250102733772
-933.333333333328	11.8394992222929	11.8394992222929	11.8394992222929
-816.666666666662	8.69293969171006	8.69293969171006	8.69293969171006
-699.999999999995	6.38263486190539	6.38263486190539	6.38263486190539
-583.333333333328	4.68633502878888	4.68633502878888	4.68633502878888
-466.666666666661	3.44085733826508	3.44085733826508	3.44085733826508
-349.999999999994	2.52638771013185	2.52638771013185	2.52638771013185
-233.333333333327	1.85495480760719	1.85495480760719	1.85495480760719
-116.66666666666	1.36196725643723	1.36196725643723	1.36196725643723
7.27595761418343e-12	1	1	1
250.000000000007	1	1	1
500.000000000007	1	1	1
750.000000000007	1	1	1
1000.00000000001	1	1	1
1250.00000000001	1	1	1
1500.00000000001	1	1	1
1750.00000000001	1	1	1
2000.00000000001	1	1	1
2250.00000000001	1	1	1
2500.00000000001	1	1	1
2750.00000000001	1	1	1
3000.00000000001	1	1	1
3250.00000000001	1	1	1
3500.00000000001	1	1	1
3750.00000000001	1	1	1
4000.00000000001	1	1	1

4250.00000000001	1	1	1
4500.00000000001	1	1	1
4750.00000000001	1	1	1
5000.00000000001	1	1	1

C Model: k/ko=10^(-m*(stress/ref pres))
C m = 0.65x10^-3
TMODTABLE 2
5000 0

C stress	TXMOD	TYMOD	TZMOD
-3500	10592.5372517729	188.36490894898	188.36490894898
-3383.33333333333	7777.38025764418	158.185498208498	158.185498208498
-3266.66666666667	5710.40178894528	132.841366171065	132.841366171065
-3150	4192.75996684607	111.557815135086	111.557815135086
-3033.33333333333	3078.4587125933	93.6842677580398	93.6842677580398
-2916.66666666667	2260.30302714192	78.6743807659941	78.6743807659941
-2800	1659.58690743756	66.0693448007596	66.0693448007596
-2683.33333333333	1218.5218841302	55.4838599287514	55.4838599287514
-2566.66666666667	894.677811357748	46.5943581229203	46.5943581229203
-2450	656.901116476265	39.1291127126853	39.1291127126853
-2333.33333333333	482.317848223929	32.8599324760065	32.8599324760065
-2216.66666666667	354.133218654328	27.5951864857302	27.5951864857302
-2100	260.015956316526	23.1739464996847	23.1739464996847
-1983.33333333333	190.912046591118	19.4610678441313	19.4610678441313
-1866.66666666666	140.173741834676	16.3430584272313	16.3430584272313
-1750	102.920052719442	13.7246096100756	13.7246096100756
-1633.33333333333	75.5672004837097	11.5256828939141	11.5256828939141
-1516.66666666666	55.4838599287508	9.67906337194042	9.67906337194042
-1400	40.7380277804109	8.12830516164095	8.12830516164095
-1283.33333333333	29.9111653293169	6.82600601544709	6.82600601544709
-1166.66666666666	21.9617360020541	5.73235836946768	5.73235836946768
-1050	16.1250102733772	4.81393254000141	4.81393254000141
-933.333333333328	11.8394992222929	4.04265487362341	4.04265487362341
-816.666666666662	8.69293969171006	3.39494961581376	3.39494961581376
-699.999999999995	6.38263486190539	2.85101826750389	2.85101826750389
-583.333333333328	4.68633502878888	2.39423440152956	2.39423440152956
-466.666666666661	3.44085733826508	2.01063544025847	2.01063544025847
-349.999999999994	2.52638771013185	1.68849585948674	1.68849585948674
-233.333333333327	1.85495480760719	1.41796877266689	1.41796877266689
-116.66666666666	1.36196725643723	1.19078493972122	1.19078493972122
7.27595761418343e-12	1	1	1
250.000000000007	1	1	1
500.000000000007	1	1	1
750.000000000007	1	1	1
1000.00000000001	1	1	1
1250.00000000001	1	1	1
1500.00000000001	1	1	1
1750.00000000001	1	1	1
2000.00000000001	1	1	1
2250.00000000001	1	1	1
2500.00000000001	1	1	1
2750.00000000001	1	1	1
3000.00000000001	1	1	1
3250.00000000001	1	1	1

3500.00000000001	1	1	1
3750.00000000001	1	1	1
4000.00000000001	1	1	1
4250.00000000001	1	1	1
4500.00000000001	1	1	1
4750.00000000001	1	1	1
5000.00000000001	1	1	1

Sensor Include Data File (well.inc)

```
C GOC 13538
PINIT 5000
ZINIT 10000

ENDINIT
C -----------------------------------------------------------------
C Include recurrent data generated by SensorGrid (perforations and TZ modifiers)
C -----------------------------------------------------------------
INCLUDE
..\recurrent.inc


BHP
 PROD 1500
 INJ  8000

SKIP
THP
 PROD 100 -2
SKIPEND

WELLTYPE
 PROD MCF
 INJ  STBWATINJ

PSM


MAPSFREQ 20
MAPSFILEFREQ 20
DTMAX 1
```

Sensor Include Data File (recurrent.inc)

```
---------------------------------
C Trans. modification to fractures
C ---------------------------------
MODIFY TX 1.0
 14 14 20 20 1 5 * 1
 15 15 20 20 1 5 * 1


C ---------------------------------
C Define Wells
C ---------------------------------
WELL
          I     J     K1    K2    PI
 PROD   15    1     1     1     100
 INJ      15    1     1     1     100
```

Sensor Include Data File (schedule.inc)

```
C Injecting water slug
RATE
PROD -1
 INJ  16000

C Start of production
TIME 0.125
DT 0.01

RATE
 INJ -1

WELLTYPE
 PROD STBWAT
BHP
 PROD 1500
RATE
 PROD 100
TIME 10.125

WELLTYPE
 PROD MCF
RATE
 PROD 500
TIME 200.125
```